Coordination Chemistry Reviews, 25 (1978) 31—67

LIGAND FIELD PARAMETERS AND SPECTRA OF FIRST-ROW TRANSITION METAL DIHALIDES IN THE SOLID STATE

DAVID R. ROSSEINSKY and IAIN A. DORRITY
University of Exeter, Exeter EX4 4QD (Gt. Britain)
(Received 7 June 1977)

CONTENTS

A. INTRODUCTION

Ligand field spectra have been reported for the majority of the solid dihalides, using single crystal (SC) absorption or diffuse reflectance (DR) powder techniques, at temperatures ranging from 300—4.2 K. In several cases both techniques have been used, calling for a comparison between the two, which is not often made. Some of these studies have been included in the many reviews [10—12] of ligand field spectra of transition metal ions and in standard texts [1,13—17] but nowhere in the last five years has there appeared a comprehensive and comparative review of all the data available. Thus, as indicated herein, some grossly outdated values still have currency in papers

TABLE 1

Crystal structures [a] of first-row transition metal dihalides

	Fluoride	Chloride	Bromide	Iodide
Ti	—	CdI_2 [b]	CdI_2	CdI_2
V	Rutile	CdI_2 [b]	CdI_2	CdI_2
Cr	Distorted rutile	$CrCl_2$	$CrBr_2$	CrI_2
Mn	Rutile	$CdCl_2$	CdI_2	CdI_2
Fe	Distorted rutile	$CdCl_2$	CdI_2	CdI_2
Co	Rutile	$CdCl_2$	CdI_2	CdI_2
Ni	Rutile	$CdCl_2$	$CdCl_2$	$CdCl_2$ [b]
Cu	Distorted rutile	$CuCl_2$	$CuCl_2$	—

[a] For references to structures, bond lengths and unit cell parameters see ref. 16. [b] There is some doubt about the structures of these compounds.

and textbooks, unscathed as Dorian Gray. Furthermore, inspection of the literature reveals a wide variation in the ligand field parameters derived for a given compound by different authors. The problem is not necessarily to choose a "best" set of values, since two different approximate treatments could be equally valid, but it can sometimes be indicated that one result appears markedly less arbitrary than another.

The crystal structures of the dihalides are shown in Table 1. All the difluorides have the tetragonal rutile structure in which the metal cation is surrounded by an approximate octahedron of fluoride ions. In the case of chromium, ferrous and copper difluoride there is pronounced distortion from octahedral to approximately tetragonal symmetry generally ascribed to the Jahn—Teller effect.

The majority of the dichlorides, dibromides and diiodides adopt the cadmium dichloride or cadmium diiodide type structures. These are both layer-type structures which differ only in the packing of the halide ions. The cadmium dichloride structure is based on a cubic close-packer arrangement of halide ions with half the octahedral holes occupied by cations, whereas the cadmium diodide type structure has hexagonal close-packed arrangement exceptions are the chromium and copper dichlorides and dibromides and chromium diiodide which have chain-type structures in which the coordination about each cation is of the form of a tetragonally elongated octahedron resulting from the Jahn—Teller effect again.

All the dihalides are high spin types and with the exception of those of chromium and copper, and ferrous difluoride, they all comprise octahedrally coordinated metal cations. The series thus proves ideal for the study of the spectrochemical [1] and nephelauxetic series [1—4], lattice contractions

[5,6] and ligand—field stabilisation energies [7—9], using the parameters derived from their electronic spectra.

Liehr [88] considered the shortcomings of the ligand field theory. Although not expected to apply exactly to the observed spectra it must be emphasized that this inadequacy is not always the cause of the variation of the derived parameters, as will be seen. The main origins of the discrepancies may be listed as follows.

B. MAIN SOURCES OF ERROR IN FITTING PARAMETERS TO SPECTRA USING LIGAND FIELD THEORY

The errors can be ascribed to one or more of
(1) Differences in *observed* band positions in spectra, largely arising from well-known difficulties in diffuse reflectance spectroscopy.
(2) Different assignments of observed bands.
(3) Parameters derived by fitting to zero-phonon transitions.
(4) Parameters derived by fitting to room-temperature rather than low-temperature spectra.
(5) Differing methods used in calculating parameters.

Points (1) and (2) are self-explanatory and need no further elaboration but points (3)—(5) will be discussed in more detail below where one or two key references will be quoted. Complete citations to assignments will be given in the subsequent detailed survey of each electronic configuration.

(3) In ligand field theory, all energy differences are calculated at a constant value of Dq, implying "vertical" transitions in energy-level diagrams. Since the relationship [13] $10Dq \propto r^{-5}$ holds approximately, this procedure is equivalent to assuming a fixed metal—ligand distance r. For most d—d transitions the minima of the excited and ground states do not lie at the same value of r, since the states usually originate in different strong-field configurations. In addition d—d transitions are parity forbidden but can gain intensity by coupling to an odd vibrational mode. Thus the non-phonon transition is absent or of very weak intensity and at low temperatures the observed absorption will consist of a progression of one or more even vibrations based on the vibronic origin. The most intense transition will occur when the vibrational overlap, between the $v = 0$ function of the ground state and an excited vibrational level of the excited state, is greatest. This transition corresponds to the Franck—Condon maximum of the observed absorption band and it is this maximum which must be compared with the theoretical energy [12,18]. In most cases this procedure has been followed but there have been instances when the calculated energies have been fitted to the estimated or observed energies of zero-phonon transitions (e.g. refs. 40 and 76) and this can lead to incorrect values of the computed ligand field parameters.

(4) Since spectra are in general markedly temperature dependent in both intensity and wavelength parameters derived from room temperature spectra

and those obtained from spectra at cryogenic temperatures will in general differ. Dq will increase on going from high to low temperatures since the metal—ligand distance will contract on cooling; the main temperature dependence arises because in the high temperature spectra, transitions take place from thermally populated spin—orbit or vibrational levels of the ground state whereas the transitions take place from the zero-point level at or near 0 K. This accounts for the shift in observed maxima to higher energies as the temperature is decreased. Thus in general, band maxima observed in room temperature spectra should not be compared with calculated transition energies, since the theory is best related [12,18] to transitions from the zero-point vibrational level of the ground state. Dq values for different compounds should be compared only if they were obtained at cryogenic temperatures, since the vibrational structure will in general be different from substance to substance [18], otherwise erroneous conclusions could ensue, see also [109].

(5) Some of the variation of the derived parameters for a given compound is due to the different methods of calculation used by different authors. For the d^2, d^3, d^7 and d^8 compounds the values of Dq and B are normally fixed from two of the three spin-allowed bands and the accuracy checked by calculating the energy of the band not used in the fitting. It is important that all three bands are observed, since although the parameters can be derived from two, some transitions are relatively insensitive to the choice of Dq and B. Inaccurate values can thus be obtained if they are not checked by comparison of the calculated and observed energies of the remaining transition, as has been well illustrated by König [18,19].

The value of C can then be fixed from one of the spin-forbidden transitions or by fitting to all of them. C is sometimes fixed by assuming the C/B ratio to be the same as that of the free ion. However this procedure is unjustifiable since the nephelauxetic effect does not act equally on B and C, and C is usually reduced less than B [4,12,20]. Thus the ratio C/B is expected to increase on going from the free ion to a complex. (Even for free ions the C/B ratio is not always known very accurately since the free-ion energy levels cannot be exactly fitted by a unique set of B and C values, see page 183.)

For d^4, d^6 compounds there is only one spin-allowed band and this is used to fix a value of Dq. The values of B and C are then calculated from the positions of the spin-forbidden transitions as for the d^2, d^3, d^7 and d^8 systems.

The situation for d^5 compounds is somewhat different since all transitions are spin forbidden. B and C can be fixed from the positions of two of the "Dq independent" transitions and then Dq is varied to give the best fit to the remaining observed bands. Alternatively, B, C and Dq can all be varied to give the best possible fit to all the transitions.

In some cases spin—orbit coupling has been included in the calculation of energy levels. The effect is usually small, and its inclusion does not greatly change the values of the parameters from those obtained when spin—orbit coupling is excluded. The two exceptions are the cases of octahedral Co^{2+} and Ni^{2+}, where spin—orbit coupling is important. For the case of Co^{2+}, spin—

orbit coupling produces an overall splitting of the ground state $^4T_{1g}$ (^4F) of about 1000 cm^{-1}. In Ni^{2+} complexes [94,95] the splitting of the $^3T_{2g}(^3F)$, $^3T_{1g}(^3F)$ and $^3T_{1g}(^3P)$ excited states is appreciable and in some cases the components are resolvable. Thus differences between parameters calculated with spin—orbit coupling and those obtained without are only to be expected for the cobalt and nickel dihalides.

The totality of these considerations emphasizes that any comparison made of the parameters of one compound with those of another is of little significance unless care is taken to ensure that the parameters were derived in corresponding ways. Even greater caution should be exercised when comparing the values of the Racah parameters obtained for a given compound with those obtained for the free ion, since the choice of B and C for a given ion is fairly arbitrary because the states of the free ion cannot be described accurately using a unique set of values for B and C, and a wide range of values can be found in the literature (e.g. cf. refs. 13, 15, 17). In order to obtain a useful comparison the same method must be used to obtain B and C in the free ion and in the complexed ion [12].

The reasons for the inadequacies of the Slater—Condon—Shortley or Racah formalisms in calculating the energy levels of the free ion are well known and understood. These discrepancies arise from the neglect [12,88,104] of configuration interaction with higher lying terms such as $d^{n-1}s^1$. The theory can be improved by the inclusion of the Trees correction [12] in each expression for the term energy but in some cases the deviations from these corrected energies are still large [12], e.g. the ^2P term is experimentally observed to be the lowest lying doublet state for Cr^{3+} but the theory predicts the ^2G term to be the lowest.

These deficiencies in representing the free ion states will be carried over when the ion is in a ligand field. The inclusion of the Trees correction in the weak field matrices would result in more accurate calculations, but in the case of the dihalides this procedure [53,55,60,62] has only been carried out for MnF_2, $MnCl_2$ and $MnBr_2$. For the majority of the dihalides the strong field scheme was used and the Trees correction cannot be easily incorporated into these matrices.

However, as discussed above, even the inclusion of the Trees correction does not always result in an adequate description of the free ion. Therefore the best approach seems to be that suggested by Ferguson [12] where rather than use the theoretical expressions for the free ion energies in the weak field matrices, the experimental free ion energies, appropriately adjusted [12] (reduced) for the best fit to the spectra of the compounds, are substituted instead. (The adjustment is constrained by having to fit the manifold resulting from the ligand field splitting). This modification cannot be made to the strong field matrices since the off-diagonal elements contain the interelectronic repulsion contributions, whereas the weak field matrices are diagonal in the energy of the free ion.

Unfortunately this scheme has not been used in the calculation of the

energy levels of any of the transition metal dihalides, although Ferguson et al. successfully used it for various d^3, d^5, d^6, d^7 and d^8 complexes [12,21—24,87]. Thus until these calculations are performed for the dihalides, using low temperature spectral data, it is difficult in most cases to obtain a clear unambiguous picture of the variation of Dq and the interelectronic repulsion energies, and from these deduce information about the bonding in these compounds.

C. ORGANISATION OF DETAILED REVIEW SECTIONS

The remainder of the review deals principally with the assignment of the observed absorptions and the derivation of parameters from the spectra. The numerous studies of spin—wave sidebands, exchange effects and related observations in the electronic spectra of the difluorides will not be considered here, these specific phenomena being the subject of reviews elsewhere [25—29].

In the following sections the electronic spectra of the dihalides are reviewed in order of the number of 3*d* electrons they contain. Then for each metal ion the spectra of the dihalides are, in most cases, considered according to structural type; e.g. the spectra of the dichlorides, dibromides and diiodides, with the $CdCl_2$ and CdI_2 structures, are discussed together in one section, since the structures of these compounds are closely related, the spectra of the difluorides, with the rutile structure, are usually considered separately.

Apart from those of ferrous fluoride and the chromium and copper dihalides, the spectra have been analysed assuming a ligand field of octahedral symmetry. Although the symmetry of the dihalides with the $CdCl_2$ and CdI_2 structures is D_{3d}, the trigonal distortion is normally very small, as evidenced by the small deviation of the ratio of the unit-cell parameters c and a from the ideal value, as can be discerned from ref. 16. Spectral features attributable to this lower symmetry are very rarely found and so the assumption of an octahedral ligand field is justifiable.

The observed maxima (when given) and assignments made by each author are tabulated together with the derived parameters, which are discussed in the light of the arguments we have presented earlier. Where spectra have been recorded at several temperatures the tables usually refer to the measurements made at the lowest attained temperature, which is indicated together with the spectral technique used.

Parameter notation

While the more basic Condon—Shortley parameters F_2 and F_4 might be preferred to the Racah electronic repulsion parameters B and C, since in using the latter the different reductions of F_2 and F_4 from the free ion values tend to be concealed [4,12], the Racah parameters are much more commonly used. To aid comparison and reference to the literature the Racah usage is followed in this review and F_2 and F_4 as usual converted by $B = F_2 - 5F_4$, $C = 35F_4$.

Dq is the cubic field splitting parameter and Ds and Dt the tetragonal field parameters.

The one electron spin–orbit coupling constant ζ has been used and compound λ values been re-expressed as $\zeta = 2s|\lambda|$.

D. LIGAND FIELD SPECTRA OF DIHALIDES

(i) d^2 Titanium dihalides ($TiCl_2$ and $TiBr_2$)

The diffuse reflectance spectra of titanium dichloride has been measured by Clark [30] and by Fowles et al. [31] who also measured the spectrum of titanium dibromide. In both cases a region of broad absorption was observed, which was considered to arise from the promotion of delocalised electrons to a conduction type band rather than from ligand field transitions.

(ii) d^3 Vanadium dihalides (VCl_2, VBr_2 and VI_2)

Single-crystal absorption spectra [32–35] of VCl_2, VBr_2 and VI_2 have been reported at temperatures down to 5 K. Clark [30] also measured the diffuse reflectance spectrum of VCl_2 at room temperature, although only the spin-allowed bands were observed. The agreement between these spectra is good and the observed absorptions together with assignments are shown in Table 2.

Several spin-forbidden transitions were observed in the single-crystal spectra but only those below ~20 000 cm^{-1} have been definitely assigned by Smith [33] and by van Erk and Haas [35]. Their assignments are identical apart from those for the bands at 18 520 cm^{-1} in VCl_2, 17 180 cm^{-1} in VBr_2 and 15 900 cm^{-1} in VI_2. Smith [33] observed all these broad structureless absorp-

TABLE 2

Observed energy levels [a] (cm^{-1}) relative to $^4A_{2g}(^4F)$ ground state for vanadium dihalides

	VCl_2			VBr_2	VI_2	
	DR [30] RT?	SC [34] 22K	SC [32,33] [b] 4.2K?	SC [33] [b] 4.2K?	SC [33] 4.2K?	SC [35] 5K
$^4T_{2g}(^4F)$	9000	9300	9200	8600	7870	7870
$^2E_g(^2G)$	—	—	11 700	11 400	—	10 993
$^2T_{1g}(^2G)$	—	—	12 200	12 000	—	11 552
$^4T_{1g}(^4F)$	14 000	14 220	14 270	13 330	12 270	12 250
$^2T_{2g}(^2G)$	—	—	16 100	15 800	15 060	15 022
$^2A_{1g}(^2G)$	—	—	18 520 [c]	17 180 [c]	—	17 000
$^2T_{2g}(^2H)$	—	—	20 790	—	—	—
$^2T_{1g}(^2H)$	—	—	—	—	—	—
$^4T_{1g}(^4P)$	21 500	22 244	22 940	20 330	18 920	19 300

[a] Higher energy bands have been observed but have not been assigned. [b] Some assignments are from ref. 35. [c] Assigned to two-centre excitation $^4A_{2g}(^4F) + {}^4A_{2g}(^4F) \rightarrow {}^4T_{2g}(^4F) + {}^4T_{2g}(^4F)$ by Smith [33].

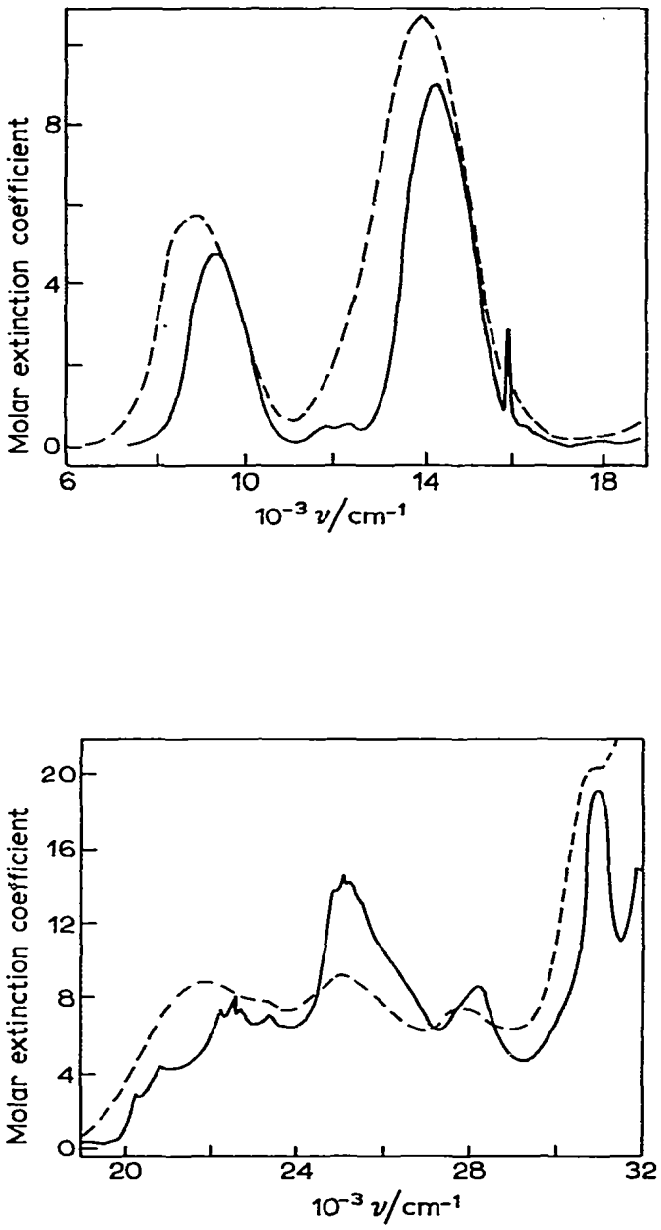

Fig. 1. Absorption spectrum of VCl_2: dashed, 298 K; solid trace, 22 K [34].

tions, whose intensities increased with decreasing temperature, and assigned them to a two-centre excitation $^4A_{2g}(^4F) + {}^4A_{2g}(^4F) \rightarrow {}^4T_{2g}(^4F) + {}^4T_{2g}(^4F)$, since their peak values lie at approximately twice that of the $^4A_{2g}(^4F) \rightarrow {}^4T_{2g}(^4F)$ transition. However van Erk and Haas [35] did not observe the 15 900 cm^{-1} band in their study of VI_2 and they maintain that the absorptions in VCl_2 and VBr_2 can be assigned to the spin-forbidden transition $^4A_{2g}(^4F) \rightarrow {}^2A_{1g}(^2G)$ which is expected to be broad, since the energy separation between the two levels is strongly Dq dependent.

The spin-forbidden transitions in VCl_2, VBr_2 and VI_2 appear to be of high intensity, particularly those above 20 000 cm^{-1}, and some show an anomalous temperature dependence. Unfortunately no detailed studies of the dependence have been made, although van Erk and Haas [35] observed a decrease in intensity and the appearance of fine structure in the bands corresponding to the transitions to the $^2E_g(^2G)$, $^2T_{1g}(^2G)$ and $^2T_{2g}(^2G)$ levels, in VI_2, as the temperature was lowered through the Néel point [35] (T_N = 15 K) below which the compound is magnetically ordered. Smith [33] observed an increase in intensity as the temperature was lowered (300—5 K) for the corresponding transitions in VCl_2 and VBr_2. It might seem that for both these compounds all measurements were made below the Néel points T_N (VCl_2 700 K, VBr_2 400 K) but these are 1941 values [105] doubtless in need of revision since for VI_2 T_N was then [105] given as 100 K.

The cause of the high intensity and the anomalous temperature dependence of the spin-forbidden transitions in the vanadium dihalides is not clear. Kim et al. [34] consider that the high intensity of the transitions above $\simeq$ 20 000

TABLE 3

Ligand field parameters for vanadium dihalides (Parentheses indicate source of measurement if different from ref.)

	Ref.	Temp.	Dq (cm^{-1})	B (cm^{-1}).	C (cm^{-1})	C/B
VCl_2	30	RT?	900	606	—	—
	34	22	800 [a]	755 [b]	—	—
	33 [c]	4.2?	920	615	2410	3.92
	19(34)	22	930	571	—	—
	35(33)	4.2?	920	610	2390	3.9
	35(33)	4.2?	920	575	2473 [d]	4.3 [d]
VBr_2	33 [c]	4.2?	860	530	2550	4.81
	35(33)	4.2?	860	568	2430	4.3
	35(33)	4.2?	860	565	2430 [d]	4.3 [d]
VI_2	33 [c]	4.2?	790	510	2450	4 80
	35	5	787	530	2370	4.5
	35	5	787	540	2322 [d]	4.3 [d]

[a] Dq calculated from estimated position of zero-phonon transition for $^4A_{2g}(^4F) \rightarrow {}^4T_{2g}(^4F)$ band. [b] Free ion value used. [c] Spin—orbit coupling included, ζ = 140 cm^{-1}. [d] C/B held constant at free-ion value and B varied to give best fit to observed quartet and doublet levels.

cm^{-1} in VCl_2 arises from intensity stealing from the higher energy parity-allowed charge transfer states. The cooperative intensity mechanism [36] provides another possible explanation for these observations [33,35].

The parameters derived by different authors are shown in Table 3 and reasonable agreement is found for those derived from low temperature spectra for each dihalide, apart from those for VCl_2 given by Kim et al. [34]. König [19] has pointed out that these are incorrect since they were obtained by fitting to the estimated energies of the zero-phonon lines of the spin-allowed transitions (see p. 181).

(iii) d^4 Chromium dihalides

(1) CrF_2. The room-temperature diffuse reflectance spectrum of CrF_2 has been recorded by Clark [30], Fackler and Holah [37] and Oelkrug [38,39]. Polarised single crystal absorption spectra of CrF_2 have been obtained by Lim and Stout [40] at temperatures down to 5.5 K, and Holloway and Kestigan [41] have studied the single crystal spectrum at room temperature and 77 K. Only the spin-allowed bands were observed by Clark [30] and Fackler and Holah [37]. However, the spectrum reported by Clark indicates [37,38] that his sample was considerably contaminated by Cr(III) (the intense broad band [30] at 23 000 cm^{-1} is probably a spin-allowed band of Cr^{3+}). The other measurements also revealed the presence of several sharp bands in the visible region which were assigned to spin-forbidden transitions.

CrF_2 has a distorted-rutile-type structure in which CrF_6 octahedra are elongated and have the two axial Cr—F bonds appreciably longer than the four equatorial bonds [42]. The deviation from O_h symmetry is attributable to Jahn—Teller distribution (a non-linear molecule in a degenerate orbital state may distort in order to remove the degeneracy). In a ligand field of octahedral symmetry a d^4 high spin complex such as CrF_2 has the degenerate ^5E_g ground state and so this interacts with an e_g vibrational mode which results in a considerable energy gain for the D_{4h} symmetry over the O_h symmetry, manifested in a static distortion [39]. In fact the symmetry at the position of the Cr^{2+} ion in CrF_2 is only C_{2h} but approximates closely to D_{4h}.

In order to assign the spin-allowed transitions for CrF_2 a D_{4h} term diagram must therefore be used. Definite assignments have only been attempted by Oelkrug [38,39] and by Lim and Stout [40] but their respective assignments differ considerably.

In a ligand field of D_{4h} symmetry the ^5D term of the free Cr^{2+} ion is split [14,39] into four quintet states — $^5A_{1g}$, $^5B_{1g}$, $^5B_{2g}$ and ^5E_g as shown in Fig. 2. The B_{1g} term is predicted [39] to be the ground state, since the octahedron is elongated and thus three spin-allowed transitions from this state to the other quintet levels are to be expected. Their energies are given by the expressions in Table 4 in terms of the octahedral splitting parameter Dq and the tetragonal splitting parameters Ds and Dt.

The energy order of the excited states given by Oelkrug [38,39] is A_{1g}

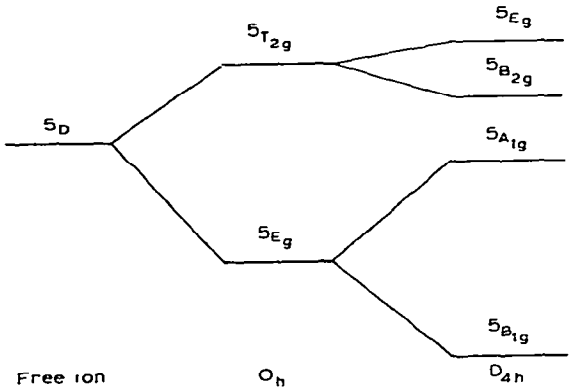

Fig. 2. Splitting of d^4 ^5D term in O_h and D_{4h} (elongated along z axis) ligand fields. (Not to scale) (Contrast ref. 40: see text).

$< B_{2g} < E_g$ and Lim and Stout [40] give $A_{1g} < E_g < B_{2g}$. However, Oelkrug considers that the B_{2g} state is extremely unlikely to lie above the E_g state, since in the electrostatic model this could only occur at very small metal—ligand distances and using a covalent model it is predicted to be impossible.

Lim and Stout consider the A_{1g} level to lie approximately 100 cm^{-1} above the ground state. This value was obtained from heat capacity measurements which suggested that there were two low-lying orbital levels. whereas Oelkrug estimates the $^5B_{1g} \rightarrow {}^5A_{1g}$ transition to lie at $\simeq$ 9000—10 000 cm^{-1}, in accordance with his observations on $KCrF_3$, $NaCrF_3$ and Na_2CrF_4. Also the splitt-

TABLE 4

Splitting parameters, observed energies and theoretical formulae of spin-allowed transitions of chromium difluoride.

Transition	Theoretical formula	Observed (cm^{-1})	
		Ref. 40 [a]	Refs. 33, 39 [b]
$^5B_{1g} \rightarrow {}^5A_{1g}$	$4Ds + 5Dt$	119 [c]	$\simeq$9000—10 000 [d]
$^5B_{1g} \rightarrow {}^5B_{2g}$	$10Dq$	10 394 [e]	10 950
$^5B_{1g} \rightarrow {}^5E_g$	$10Dq + 3Ds - 5Dt$	7677 [f]	14 300
Dq		1039.4	1095
Ds		−371	$\simeq$1700 [g]
Dt		320	$\simeq$450 [g]

[a] 5 K spectrum. [b] RT spectrum. Bands at 11 400 and 14 700 cm^{-1} observed in RT spectrum by Clark [30] and at 11500 and 14 700 cm^{-1} by Fackler and Holah [37]. [c] Calculated from heat capacity measurements. [d] Estimated by comparison with other Cr(II) fluorides but not observed, although a band at 9859 cm^{-1} was observed in RT spectrum by Lim and Stout [40]. [e] Magnetic dipole line. [f] Calculated position. [g] Estimated by comparison with other Cr(II) fluorides.

ing of the ^5E_g (in O_h) ground state, by the Jahn—Teller distortion, which corresponds to the $^5B_{1g} \rightarrow {}^5A_{1g}$ transition, has been calculated by Liehr and Ballhausen [43] to be approximately 6000 cm^{-1}.

The room-temperature spectra in the near IR region are all qualitatively similar and consist of a broad absorption with two maxima, B2 and B3 (Lim and Stout's arbitrary labels) in order of increasing energy. However Lim and Stout [40] were able to resolve a further maximum B1, on the low energy side of B2, using a Gaussian analysis, but Oelkrug was unable to resolve this absorption.

In addition to these three broad maxima a sharp line, half-width 4 cm^{-1} was also observed between B1 and B2 in the 6.5 K single-crystal spectrum, and it was identified from its polarisation properties as a magnetic dipole line [40]. This was assigned to the origin of the $^5B_{1g} \rightarrow {}^5B_{2g}$ transition and B2 was considered to contain the remaining magnetic dipole and electric dipole contributions for this transition. The bands B1 and B3 were assigned to combinations of the ^5E_g electronic state, which was calculated to lie slightly below the beginning of B1, with vibrational modes.

Oelkrug assigned B2 and B3 to transitions to the $^5B_{2g}$ and ^5E_g states respectively but was unable to assign the $^5B_{1g} \rightarrow {}^5A_{1g}$ transition since (see above) the band B1 was not resolved by him.

This drastic disagreement in assignments obviously is reflected in the parameters derived from the spectra, using the energy level separations in Table 4. Since Oelkrug only observed two quintet—quintet transitions, only the one parameter Dq could be calculated, but estimates of the values of Ds and Dt can be made from consideration of the spectra of the other Cr(II) fluorides studied by him. Lim and Stout fixed their value of Dq from the energy of the magnetic dipole line of the transition to the $^5B_{2g}$ level, and Ds and Dt were determined using the results of heat capacity measurements, and by diagonalising the ^3E_g and $^3B_{2g}$ matrices for a d^5 ion in a D_{4h} ligand field to give the best fit to the observed spin-forbidden transitions. The values of the Racah parameters B and C used in these matrices were those derived from the free-ion spectrum of Cr^{2+} and were not reduced, as is the normal practice, to account for the reduction of the interelectronic repulsion energies on complex formation.

The derived parameters are shown in Table 4, and it is of interest to note that the tetragonal splitting parameters Ds and Dt obtained by Lim and Stout are of opposite sign, whereas those obtained by Oelkrug both have positive values. The electrostatic model, used to calculate the energy level separations, allows only that Ds and Dt should both have the same sign [39] and in the case of an elongated octahedron such as CrF_2 should both be positive (if the octahedron is compressed they are predicted to be negative). However, insistence on the identity of signs for Ds and Dt has been suggested [4] to be "a too-literal adherence to the point-charge model" in the case of mixed ligands.

The observed sharp spin-forbidden transitions are all in reasonable agreement. However their assignments do differ, as shown in Table 5. Oelkrug [38]

TABLE 5

Observed energies (cm^{-1}) and assignments of spin-forbidden transitions in chromium difluoride

Assigned on basis of O_h symmetry				Assigned on basis of D_{4h} symmetry [a]	
SC [41] (77 K)		DR [38] (RT.?) [b]		SC [40] (6 K) [c]	
16 970	$^3E_g(^3H)$	16 920	$^3E_g(^3H)$	16 986	$^3E_g(^3H)$
		17 400	$^3T_{1g}(^3H)$		
				18 122	$^3E_g(^3H)$
18 640	$^3T_{2g}(^3H)$	18 600	$^3T_{2g}(^3H)$	18 690	$^3B_{1g}(^3F)$
19 160	$^3A_{1g}(^3G)$	19 200		19 250	$^3A_{1g}(^3G)$
				19 350	
20 200	$^3A_{2g}(^3F)$	20 170	$^3A_{1g}(^3G)$	20 270	$^3B_{2g}(^3H)$
				21 690	$^3B_{1g}(^3G)$
		23 000 [d]	$^3E_g(^3G)$		
				24 310	$^3E_g(^3P)$
				24 830	$^3E_g(^3F)$

[a] In a D_{4h} ligand field the octahedral terms are further split: $^3T_{1g} \rightarrow {}^3E_g + {}^3A_{2g}$; $^3T_{2g} \rightarrow {}^3E_g + {}^3B_{2g}$; $^3E_g \rightarrow {}^3A_{1g} + {}^3B_{1g}$; $^3A_{2g} \rightarrow {}^3B_{2g}$; $^3A_{1g} \rightarrow {}^3A_{1g}$. [b] Levels calculated using $Dq = 1110\ cm^{-1}$, $B = 770\ cm^{-1}$, $C = 3290\ cm^{-1}$. [c] Levels calculated using $Dq = 1039.4\ cm^{-1}$, $Ds = -371\ cm^{-1}$, $Dt = 320\ cm^{-1}$ and free-ion values of Racah parameters $B = 895\ cm^{-1}$, $C = 3152\ cm^{-1}$. [d] Possibly due to Cr^{3+} impurity [38].

and Holloway and Kestigan [41] assigned the transitions on the basis of an O_h ligand field since it was assumed that the energies of the triplet levels are affected by the distortion of the octahedron in a similar way to the ground state $^5B_{1g}$, and also the further splitting of the O_h terms in the tetragonal field was ignored. This procedure was justified by the good agreement obtained between the observed and computed levels. Lim and Stout [40], however, calculated the energy levels of the triplet levels in a field of D_{4h} symmetry and made their assignments on this basis, but in some cases large differences were found between the energies of observed and predicted levels.

In every case the lowest spin-forbidden transition to the $^3T_{1g}$ level, which is split into $^3A_{2g}$ and ^3E_g in D_{4h} symmetry, was not observed; measurements were made [40] down to 700 cm^{-1}. Since this transition is interconfigurational it may be too broad and weak to be observed or is possibly hidden beneath the spin-allowed transitions.

Since the triplet terms of the free Cr^{2+} ion are not fitted at all accurately by the theoretical expressions in terms of the Racah parameters, it would seem advisable to use Ferguson's free-atom method [12] (p. 183) to calculate the energies of the spin-forbidden transitions. However the weak-field matrices are only available for a d^4 ion in an O_h field and not in a D_{4h} field. When these latter matrices have been derived it would be possible to substitute the reduced term energies directly into them and to ascertain whether the spin-forbidden transitions are calculated more accurately. This may help to decide

TABLE 6

Observed maxima (cm^{-1}) in $CrCl_2$ spectrum [a] at 77 K

Spin-allowed transitions	Spin-forbidden transitions
8750, 12 000 [b]	16 300, 17 500, 19 000

[a] Diffuse reflectance measurements [37]. [b] Clark [30] reports a band at 11 400 cm^{-1} in spectrum at liquid nitrogen temperature.

which of the two totally different sets of splitting parameters derived for CrF_2 is correct, and thus confirm the assignment of the spin-allowed transitions.

(2) $CrCl_2$. Only the diffuse reflectance spectrum of $CrCl_2$ has been reported, and Clark [30] and Fackler and Holah [37] recorded the spectrum at room and liquid nitrogen temperatures. Two broad maxima corresponding to spin-allowed bands and several sharp spin-forbidden transitions, as shown in Table 6, were observed by Fackler and Holah [37]. However Clark [30] did not observe these sharp bands but his spectrum indicates [37] that his sample was contaminated with chromium(III), as for CrF_2.

The structure of chromium dichloride consists of densely packed chains of elongated and slightly distorted $CrCl_6$ octahedra [44—46]. Thus the spectrum should be qualitatively similar to CrF_2 and the assignment of the transitions should be made on the basis of a ligand field of D_{4h} symmetry. However no analysis of the spectrum has yet been attempted.

(iv) d^5 Manganese dihalides (MnF_2, $MnCl_2$, $MnBr_2$ and MnI_2)

The electronic spectra of manganese dihalides have been the subject of the greatest number of studies of all the first-row transition metal dihalides. In particular there have been numerous theoretical and experimental studies of the magnon sidebands of the transitions to the quartet levels in MnF_2. However, being outside our scope, these will not be discussed here.

In each dihalide the Mn^{2+} ion is surrounded by an approximate octahedron of halide ions. The actual symmetry at the Mn^{2+} ion is D_{2h} in MnF_2 and D_{3d} in $MnCl_2$, $MnBr_2$ and MnI_2. Since the distortion is small in every case. the spectra are qualitatively similar and can be analysed together, as for an octahedral field of anions.

The ground state of the Mn^{2+} ion in a field of octahedral symmetry is $^6A_{1g}(^6S)$. This is the only sextet level and thus only spin-forbidden transitions to the quartet levels derived from the ^4G, ^4D, ^4P and ^4F excited states are expected. In addition doubly spin-forbidden transitions are possible to levels arising from the doublet states of the free ion, but these are predicted to be of extremely low intensity and have only been reported for $MnCl_2$.

Room-temperature diffuse-reflectance spectra and single-crystal spectra

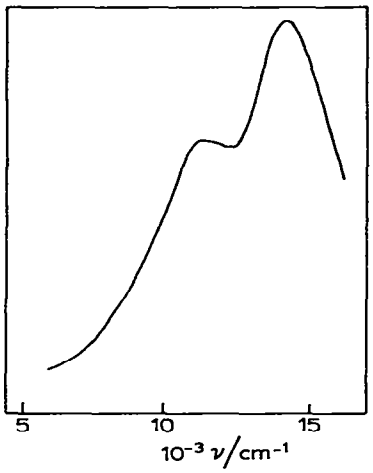

Fig. 3. Reflectance spectrum of CrF_2 (quintet—quintet transitions only) at room temperature [38,39].

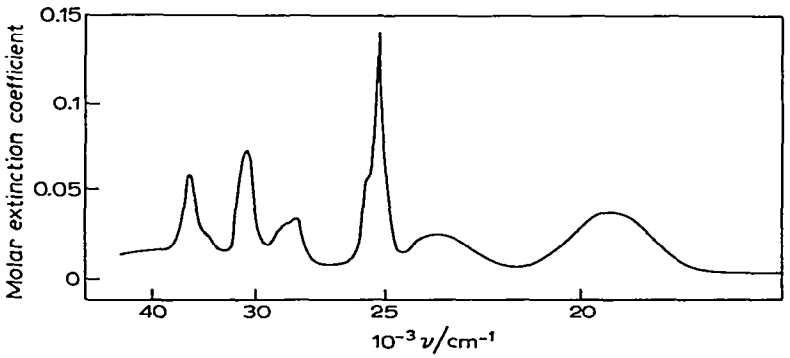

Fig. 4. Absorption spectrum of MnF_2 at room temperature [47].

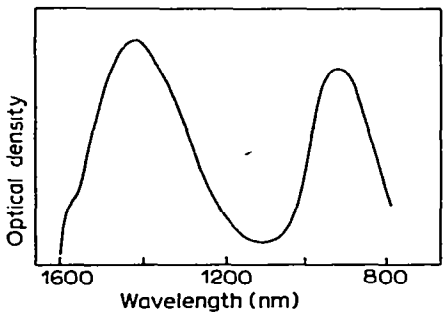

Fig. 5. Absorption spectrum of FeF_2 in near infrared region at 77 K [64].

TABLE 7

Observed energy levels (cm^{-1}) relative to $^6A_{1g}(^6S)$ ground state for manganese difluoride

	SC [51] 300 K	SC [47] RT?	SC [52] RT	SC [53] RT
$^4T_{1g}(^4G)$	19 200	19 440	19 500	—
$^4T_{2g}(^4G)$	23 100	23 500	23 410	—
$^4A_{1g}(^4G)$	25 200	25 190 25 300	25 210 25 320	25 200 25 280
$^4E_g(^4G)$		25 500	25 500	25 570
$^4T_{2g}(^4D)$	28 200	28 120 28 370	28 150	28 000 28 150 28 340
$^4E_g(^4D)$	30 100	30 230	30 170 30 220	30 210 30 640
$^4T_{1g}(^4P)$	32 800	33 060	33 080	33 070
$^4A_{2g}(^4F)$	—	39 000 [a]	39 010 [a]	—
$^4T_{1g}(^4F)$	—	41 400 [b]	41 340 [b]	—
$^4T_{2g}(^4F)$	—	—	43 200 [c]	—

[a] Assigned [22] to double-exciton transition $^6A_{1g}(^6S) \rightarrow {}^4T_{1g}(^4G) + {}^4T_{1g}(^4G)$. [b] Assigned to $^6A_{1g}(^6S) \rightarrow {}^4A_{2g}(^4F)$ by Ferguson [22]. [c] Assigned to double-exciton transition $^6A_{1g}(^6S) \rightarrow {}^4T_{1g}(^4G) + {}^4T_{2g}(^4G)$ by Ferguson [22].

TABLE 8

Observed energy levels (cm^{-1}) relative to $^6A_{1g}(^6S)$ ground state for manganese dichloride

	DR [54] RT	DR [30] RT?	SC [49,50] 78 K	SC [55] 77 K	SC [58] 5 K
$^4T_{1g}(^4G)$	18 900	18 650	18 500	18 500	18 450
$^4T_{2g}(^4G)$	22 220	22 100	22 000	22 000	21 882
$^4A_{1g}(^4G)$	23 870	23 700	23 590	23 574 23 800	23 559
$^4E_g(^4G)$		23 900	23 825		23 792
$^4T_{2g}(^4D)$	27 030	27 040	26 750	27 000	26 998
$^4E_g(^4D)$	28 250	28 080	28 065	28 066	28 106
$^4T_{1g}(^4P)$	30 490	—	36 500 [a]	30 500	30 395
$^4A_{2g}(^4F)$	—	—	38 400	38 400	—
$^4T_{1g}(^4F)$	—	—	40 650 [b]		—
$^4T_{2g}(^4F)$	—	—	42 370 [b]	40 700 [b]	—

[a] Assigned as a transition to a doublet level by Low and Rosengarten [60]. [b] The assignment of these bands seems uncertain. It is possible they are due to transitions to doublet levels [60].

TABLE 9

Observed energy levels (cm^{-1}) relative to $^6A_{1g}(^6S)$ ground state for manganese dibromide and diiodide

	$MnBr_2$		MnI_2	
	SC [54] RT	SC [49,50] 78 K	DR [54] RT	SC [56] 5 K
$^4T_{1g}(^4G)$	18 800	18 450	18 180	17 360
$^4T_{2g}(^4G)$	21 930	21 650	21 110	20 600
$^4A_{1g}(^4G)$	23 420	23 084	22 420	22 062 [b]
$^4E_g(^4G)$		23 550		22 105 [b] 22 373 [b]
$^4T_{2g}(^4D)$	26 740	26 520	25 900	25 420 [b]
$^4E_g(^4D)$	27 630	27 505	26 450	26 338 [b]
$^4T_{1g}(^4P)$	29 760 [a]	29 950 [a]	28 900	28 920
$^4A_{2g}(^4F)$	—	34 800 [a]	—	—
$^4T_{1g}(^4F)$	—	37 400 [a]	—	—
$^4T_{2g}(^4F)$	—	38 750 [a]	—	—

[a] Van Erk and Haas [56] assigned the bands at 29 950 and 34 800 cm^{-1} to the transition to the $^4T_{1g}(^4P)$ level, and the bands at 37 400 and 38 750 cm^{-1} to transitions to the $^4A_{2g}(^4F)$ and $^4T_{1g}(^4F)$ levels respectively. [b] Zero phonon lines.

down to cryogenic temperatures have been recorded for each compound [22,30,36,47—58]. All the observed spectra are in good agreement for each dihalide as shown in Tables 7—9, and the diffuse reflectance correspond well with the single-crystal transmittance studies. However, there are disagreements and inconsistencies in the assignments of the higher-energy absorptions.

In the spectrum of MnF_2 a band at 39 000 cm^{-1} was assigned to a transition to the $^4A_{2g}(^4F)$ level by Stout [47] and by Finlayson et al. [52]. However Ferguson [22] has pointed out that this assignment is incorrect since, on cooling of the crystal, the band shifts to lower energy and thus behaves as if the excited ligand field state has a negative ligand field dependence. This is incompatible with the assignment of the band to a transition to the $^4A_{2g}(^4F)$ state, since the energy of this state should be independent of the ligand field. The absorption was instead assigned [22] to the two-exciton-transition $^6A_{1g}(^6S) \rightarrow {}^4T_{1g}(^4G) + {}^4T_{1g}(^4G)$, which is expected to occur at approximately twice the energy of the $^6A_{1g}(^6S) \rightarrow {}^4T_{1g}(^4G)$ transition. (Double-exciton transitions arise from the simultaneous excitation of two exchange coupled Mn^{2+} ions, to quartet levels. This process causes the breakdown of the spin selection rule and thus gives rise to anomalously intense bands). The assignment of this transition has been confirmed by Tanabe and co-workers [59], who measured the temperature dependence of the oscillator strength of the absorption and found a large increase in intensity as the temperature was decreased below the Néel temperature, T_N = 67.8 K, in accordance with the theoretical model.

The band at 43 200 cm^{-1} previously attributed to a transition to the $^4T_{2g}(^4F)$ state, by Finlayson et al. [52], was similarly assigned to the double-exciton transition $^6A_{1g}(^6S) \rightarrow {}^4T_{1g}(^4G) + {}^4T_{2g}(^4G)$ by Ferguson [22]. In addition he assigned the band at $\simeq$ 41 400 cm^{-1}, previously identified [47,52] as the $^6A_{1g}(^6S) \rightarrow {}^4T_{1g}(^4F)$ transition, to the $^6A_{1g}(^6S) \rightarrow {}^4A_{2g}(^4F)$ transition which was calculated by him to lie at $\simeq$ 41 000 cm^{-1}.

For $MnCl_2$, Pappalardo's [49,50] original assignment of the $^6A_{1g}(^6S) \rightarrow {}^4T_{1g}(^4P)$ transition is in error as pointed out by Low and Rosengarten [60], who from theoretical calculation assigned the band at 36 500 cm^{-1} to a transition to a doublet level. An additional band at $\simeq$ 30 500 cm^{-1}, not observed by Pappalardo, has since been assigned by several authors [54,55,57] to the $^6A_{1g}(^6S) \rightarrow {}^4T_{1g}(^4P)$ transition. In addition there are also differences in the assignment of the bands observed above 38 000 cm^{-1} by Mehra [55] and Pappalardo [49,50]. But it is also possible that the absorptions in this region are due to transitions to doublet levels [60].

In $MnBr_2$ there are doubts about the assignments of the transitions to the $^4T_{1g}(^4P)$, $^4A_{2g}(^4F)$, $^4T_{1g}(^4F)$ and $^4T_{2g}(^4F)$ levels. The spectral region in which these transitions are predicted to occur has only been studied by Pappalardo [49,50] who assigned the four observed absorptions to these transitions. However van Erk and Haas [56] have differently assigned these four bands in Pappalardo's spectrum. In neither case do the calculations give a good description of these bands and the possibility that some of them are due to transitions to doublet states should not be discounted [56]. The measurement of the oscillator strength of these bands should help clarify the position.

Table 10 shows the wide variety of parameters that have been derived from the spectra of the manganese dihalides. Also included in Table 10 is a selection of the values of the Racah parameters that have been used to fit the spectrum of the free-ion Mn^{2+}. None of these sets of values fit the observed free-ion spectrum very satisfactorily and it is only with the inclusion of Trees' correction α that the observed levels are well described [62]. Thus an accurate calculation of the ligand field states in the manganese dihalides can only be expected when the Trees correction is included.

Several procedures have been followed in order to fit the observed spectra. (1) Dq, B and C are all varied. (2) B and C are fixed at their free-ion values and Dq and a covalency parameter [108] ϵ are adjusted. The covalency parameter can be used to include the differential expansion of the t_{2g} and e_g orbitals, or the radial wave functions of the t_{2g} orbitals can be taken as being equivalent to those of the free ion and the effect of covalency restricted to the expansion of the e_g orbitals. (3) B, C, Dq and ϵ are all varied to give the best fit.

The principal advantage of the covalency parameter is that its use allows the removal of the accidental degeneracy of the $^4A_{1g}(^4G)$ and $^4E_g(^4G)$ levels which occurs using procedure (1) and which is not observed experimentally. It has been used in calculations for MnF_2, $MnCl_2$ and $MnBr_2$ by Stout [47,48]. Pappalardo [49,50], Russell and Hedges [63] and by Curie et al. [62]. How-

TABLE 10

Ligand field parameters for Mn^{2+} free ion and manganese dihalides (Parentheses indicate source of measurement if different from ref.)

	Ref.	Dq (cm^{-1})	B (cm^{-1})	C (cm^{-1})	C/B	α (cm^{-1})	ϵ
Free ion	61	0	860	3853	4.48	0	0
	13	0	960	3325	3.46	0	0
	47	0	950	3280	3.45	0	0
	62 [a,b]	0	918	3273	3.57	65 [c]	0
MnF_2	47	780	950 [c]	3280 [c]	3.45 [c]	0	0.064
	53 [d]	789	917 [c]	3271 [c]	3.57 [c]	66.1 [c]	0.0645
	62(47) [d]	828	908	3237	3.57	65 [c]	0.061
	63(47)	851	920 [c]	3227 [c]	3.51	0	0.065
	60(47) [e]	750	820	3150	3.84	76 [c]	0
	60(47) [e]	752	801	3158	3.94	76 [c]	0
	51	830 [f]	—	—	—	—	—
	22	750	700	3650	5.21	0	0
	52	820	671	3710	5.53	0	0
	54(47)	750	825	3346	4.06	0	0
$MnCl_2$	48(49)	830	950 [c]	3280 [c]	3.45 [c]	0	0.13
	62 [d]	787	896	3319	3.57	65 [c]	0.116
	63(49, 50)	896	920 [c]	3227 [c]	3.51	0	0.128
	49, 50	750	700	3430	4.90	0	0.03
	60 (49, 50) [e]	740	700	3150	4.50	76 [c]	0
	60(49,50) [e]	763	758	3082	4.07	76 [c]	0
	55	670	770	2900	3.77	76 [c]	0
	54	620	770	3132	4.07	0	0
	56(49, 50)	770	684	3352 [g]	4.9 [g]	0	0
$MnBr_2$	48(49)	940	950 [c]	3280 [c]	3.45 [c]	0	0.15
	62(49, 50) [d]	645	788	2808	3.57	65 [c]	0.009
	63(49, 50)	891	920 [c]	3227 [c]	3.51 [c]	0	0.148
	49, 50	700	700	3430	4.9	0	0.05
	54	580	721	3158	4.38	0	0
	56 (49,50)	680	669	3278 [g]	4.9 [g]	0	0
MnI_2	54	550	689	3022	4.39	0	0
	56	640	640	3136 [g]	4.9 [g]	0	0

[a] Racah seniority parameter [107] $\beta = -131$ cm^{-1} also included in fitting of free-ion spectrum. [b] Stevenson [53] has fitted free-ion spectrum using parameters almost identical to these. [c] Free-ion value used. [d] Free-ion value of β used in fitting spectrum. [e] Spin—orbit coupling included; $\zeta = 320$ cm^{-1} for $MnCl_2$, $\zeta = 240$ cm^{-1} for $MnBr_2$. [f] Dq determined from Orgel diagram. [g] C fixed equal to 4.9 B.

ever the sequence of ϵ values is not always $\epsilon(MnF_2) < \epsilon(MnCl_2) < \epsilon(MnBr_2)$ as expected from chemical considerations. Also the sequence of Dq values differs in some cases from that predicted by the spectrochemical series, $Dq(MnF_2) > Dq(MnCl_2) > Dq(MnBr_2)$. The derived Dq and ϵ values are shown in Table 10, and the sequences summarised in Table 11.

In all four cases in Table 11 the same spectral data were used in the fitting

TABLE 11

Sequences of Dq and ϵ obtained using covalent bonding type calculations

Dq Sequence	ϵ Sequence	Ref.
$MnBr_2 > MnCl_2 > MnF_2$	$MnF_2 < MnCl_2 << MnBr_2$	47, 48
$MnCl_2 > MnBr_2$	$MnCl_2 < MnBr_2$	49, 50
$MnCl_2 > MnBr_2 > MnF_2$	$MnF_2 < MnCl_2 < MnBr_2$	63
$MnF_2 > MnCl_2 > MnBr_2$	$MnBr_2 < MnF_2 < MnCl_2$	62

procedures. For MnF_2 the spectrum obtained by Stout [47] was fitted and for $MnCl_2$ and $MnBr_2$ the data was from Pappalardo [49,50]. Although there are errors and uncertainties in the assignments of the spectra of these compounds, as discussed previously, these do not affect the values of the parameters, apart from those derived by Curie et al. [62], since the wrongly and uncertainly assigned bands were not included in the fitting procedure. Curie et al. [62] were unaware of the reassignments of the higher-energy bands in MnF_2 published some six years earlier by Ferguson [22], and since the energies of the transitions to the $^4A_{2g}(^4F)$ and $^4T_{1g}(^4F)$ levels were included in the fitting, their derived parameters are thus in error, for MnF_2. Similarly their parameters derived for $MnCl_2$ and $MnBr_2$ may need to be revised when the assignments of the transitions to the $^4A_{2g}(^4F)$, $^4T_{1g}(^4F)$ and $^4T_{2g}(^4F)$ levels are confirmed, since some of the bands in this spectral region may be due to transitions to doublet states [60]. However the correct assignment of the $^6A_{1g}(^6S) \rightarrow {}^4T_{1g}(^4P)$ transition in $MnCl_2$ *was* included in their calculations and so was not a source of error.

Stevenson [53] also used the covalency parameter in fitting his spectrum of MnF_2 and obtained very similar parameter values to those derived by Stout [47,48].

All the remaining sets of parameters in Table 10 were derived using procedure (1). In addition the Trees correction was also included in the fitting of the spectrum of $MnCl_2$ by Mehra [55] and by Low and Rosengarten [60] for MnF_2 and $MnCl_2$. These last named authors also included spin—orbit coupling in their calculations, but its effect is almost negligible in Mn^{2+} compounds.

The parameters derived by van Erk and Haas [56] from the spectrum of $MnCl_2$ obtained by Pappalardo [49,50] are in error since Pappalardo's wrong assignment of the transition to the $^4T_{1g}(^4P)$ level was included in their fitting. It seems that these authors were unaware of the correct assignment; their paper was published in 1975, eleven years after the error was first pointed out [60] and seven years after the transition was first correctly identified [54,55]. (The correction was re-asserted [62], apparently de novo, in 1974).

In conclusion, the broad spread of parameter values derived for each dihalide does not arise from differences in the observed spectra, but is simply a consequence of incorrect assignments and the neglect of the Trees correction.

Apart from the set of values for $MnCl_2$ from ref. 55 in Table 10, no other set stands out as being totally free of reservations. There is thus a clear need for revised fittings, employing either the Trees term or the Ferguson free-atom treatment [12].

(v) d^6 Iron dihalides

(1) FeF_2. Single-crystal spectra of FeF_2 have been recorded at temperatures down to 4.2 K by Tylicki and Yen [64] and down to 20 K by Jones [65]. The diffuse reflectance spectrum has been obtained at room temperature by Brokopf et al. [66] and the absorption spectrum of a polycrystalline mass reported by Hatfield and Piper [67]. In every case only the near IR region was studied and two extremely broad bands were observed.

FeF_2 has a distorted rutile type structure [68] in which the FeF_6 octahedra are compressed with four Fe—F distances of 2.12 Å and two of 1.99 Å. Probably resulting from Jahn—Teller distortion as for CrF_2, the actual symmetry is D_{2h} since some of the F—Fe—F angles deviate from 90°, but may be considered tetragonal for the assignment of the absorption spectrum.

In a D_{4h} ligand field the ^5D ground state term of the free Fe^{2+} ion is split [14,39] into four levels $^5B_{2g}$, ^5E_g, $^5B_{1g}$ and $^5A_{1g}$, as shown in Fig. 6. The octahedra in FeF_2 are axially compressed and so the ground state [39] is $^5B_{2g}$ and three spin-allowed transitions to the other quintet levels are expected. The low energy band has been assigned by Oelkrug [39] as a transition to the $^5B_{1g}$ level and the other as a transition to the $^5A_{1g}$ term. The $^5B_{2g} \rightarrow {}^5E_g$ transition has not been observed experimentally but has been calculated [39] to occur at 1400 cm^{-1}. The energies of these transitions are given in terms of Dq, Ds and Dt by theoretical expressions derived from an electrostatic model. In order of increasing energy the expressions are $-3Ds + 5Dt$, $10Dq$ and $10Dq - 4Ds - 5Dt$. However since only the two higher energy bands have been observed, only the parameter Dq can be evaluated.

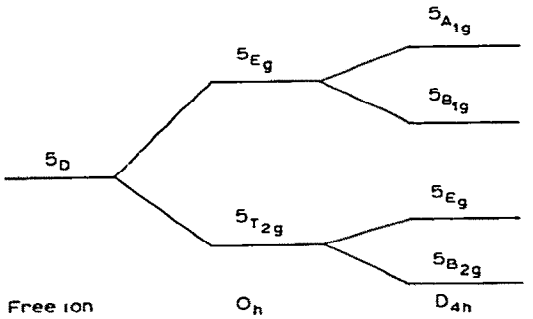

Fig. 6. Splitting of d^6 ^5D term in O_h and D_{4h} (compressed along z axis) ligand fields. (Not to scale).

TABLE 12

Observed energies (cm^{-1}) of spin-allowed bands of iron difluoride

Temp. (K)	$^5B_{2g} \rightarrow {}^5B_{1g}$ [a]	$^5B_{2g} \rightarrow {}^5A_{1g}$ [a]	Ref.
295	6990	10 600	67
290	7000	10 600	65
RT	6900	10 500	66
77	7040	10 870	64

[a] Assignments due to Oelkrug [39].

The observed spectra are all in good agreement and the maxima of the two absorption bands are shown in Table 12. In addition to these two broad bands Tylicki and Yen [64] observed a very sharp strong line with associated structure on the low energy side of the $^5B_{2g} \rightarrow {}^5B_{1g}$ band at low temperatures. From the behaviour of the sharp structure with temperature and the application of magnetic fields, it was possible to identify pure electronic transitions and 'cold' magnon sidebands [25—29,36].

(2) $FeCl_2$, $FeBr_2$ and FeI_2. The diffuse reflectance spectra of $FeCl_2$, $FeBr_2$ and FeI_2 have been recorded by Winter [69] at temperatures ranging from 363—77 K. However, these spectra are of poor quality and appear to show spurious features which may be due to the presence of hydrates as impurities. Only for $FeCl_2$ has the single crystal spectrum been recorded and Schnatterly and Fontana [70] and also Jones [65,71] have reported studies at temperatures down to 4.2 K.

Measurements were made in the near-IR region, where the spin-allowed quintet—quintet transition $^5T_{2g}(^5D) \rightarrow {}^5E_g(^5D)$ was observed in every case. However, Schnatterly and Fontana [70] also recorded the spectrum of $FeCl_2$ in the visible region and observed several spin-forbidden bands, some of which were highly structured and showed a sharp decrease in intensity below the Néel temperature $T_N = 23.5$ K. These quintet—triplet transitions could not be assigned because their observed positions did not agree at all well with the calculated spectrum. (These authors also studied the temperature dependence of the intensity of a 'hot' magnon—exciton sideband at 4270 Å associated with one of the spin-forbidden transitions. This band has since been the subject of further studies [72—74], which have also dealt with its temperature dependence and its behaviour on the application of magnetic fields).

The optical absorption spectra of $FeCl_2$, $FeBr_2$ and FeI_2 all show the spin-allowed transition $^5T_{2g}(^5D) \rightarrow {}^5E_g(^5D)$, as a broad band split into two components, as shown in Table 13. This splitting corresponds to the lowering of the degeneracy of the ^5E_g state; however the cause of this cannot be due to non-cubic ligand fields as was the case for FeF_2, since the coordination of these compounds is approximately octahedral. These halides are slightly

TABLE 13

Energies of $^5T_{2g}(^5D) \rightarrow {}^5E_g(^5D)$ transition in iron dichloride, dibromide and diiodide at $\simeq$80 K [a]

Compound	Energies (cm^{-1})	Ref.
$FeCl_2$	7470, 6500	65, 71
	7600, 6400	69
$FeBr_2$	6800, 5900	69
FeI_2	6200, 5400	69

[a] Measurements were made at other temperatures but 80 K was chosen as lowest common temperature for comparison.

trigonally distorted but trigonal fields do not split the E_g state. Spin—orbit coupling can also be rejected as the cause of the splitting since it is small for Fe^{2+} and only splits the ^5E_g state in second order.

Jones [65,71] and Winter [69] resolved the broad band into two components and studied the temperature dependence of the splittings which were found to decrease as the temperature was decreased. Being a characteristic of the dynamic Jahn—Teller effect, this mechanism was invoked to explain the splitting [65,69,71]. In these studies the high-energy component was observed to remain at approximately the same position and the lower energy component shifted markedly to higher energies with decreasing temperature.

In addition, in the single crystal measurements of $FeCl_2$, the intensities of the two different components were observed to vary differently with temperature [65,70,71]. This behaviour is puzzling since it implies that different phonons are coupled to the two states giving rise to the bands. This is not expected since the Jahn—Teller interpretation implies that the states have the same symmetry and so must couple with equal strength to other electronic states [70]. Schnatterly and Fontana [70] suggested that impurities might in some way be responsible for this effect.

Since spin-forbidden transitions have only been observed for $FeCl_2$ and these were not assigned, no values of the Racah parameters for $FeCl_2$, $FeBr_2$ and FeI_2 have been fitted. The value of Dq can be fixed from the $^5T_{2g}(^5D) \rightarrow {}^5E_g(^5D)$ transition, whose energy is equal to 10 Dq, but the splitting of this transition by the dynamic Jahn—Teller effect makes the choice a fairly arbitrary one.

(vi) d^7 Cobalt dihalides

(1) CoF_2. Cobalt difluoride has the rutile type structure in which each Co^{2+} ion is surrounded by six F^- ions distorted in angle from a regular octahedron [58]. The site symmetry of the Co^{2+} ion is D_{2h} but analysis of the electronic spectrum of CoF_2 can be carried out on the basis of an octahedral ligand field since the distortion is small.

TABLE 14

Observed energies (cm^{-1}) of quartet levels relative to ground state $^4T_{1g}(^4F)$ for cobalt dihalides

	Ref.	Method	Temp.	$^4T_{2g}(^4F)$	$^4A_{2g}(^4F)$	$^4T_{1g}(^4P)$
CoF_2	75	DR	RT	6800	14 700	18 700, 20 500
	76 [a]	SC	20.4	7300	14 450	19 050, 20 600
	77	SC	RT	7140	—	—
$CoCl_2$	75	DR	RT	6200	12 600	16 800, 18 500 [b]
	80	DR	RT	6580	—	17 100
	81	SC	20	6600	13 300	17 150, 17 350
$CoBr_2$	75	DR	RT	5700	11 800	16 000, 17 500
	80	DR	RT	6090	—	15 900
	81	SC	20	6200	12 000	16 400—17 400

[a] σ spectrum. [b] This band occurs as a shoulder and is possibly due to a transition to a doublet level.

The diffuse reflectance spectrum at room temperature has been reported by Ludi and Feitknecht [75] while the single crystal spectrum has been studied by Zimring and Stout [76] and Eremenko et al. [77,78] at temperatures down to 20.4 K. In addition there have been numerous studies, not considered further here, of the spin—wave sidebands in the ligand field transitions and their behaviour with temperature and on application of magnetic fields, e.g. refs. 28, 78, 79, 106.

All three spin-allowed transitions have been observed for CoF_2 and their assignments are shown in Table 14. The transition to the $^4T_{1g}(^4P)$ state appears to be split and strongly polarised. Zimring and Stout [76] suggested that this splitting is due to the effect of low-symmetry fields, which remove the degeneracy of this state.

Several weak spin-forbidden bands have also been observed in the crystal spectra referred to above. These have been assigned in some cases [78,79] but no attempt appears to have been made to check the assignments by calculating the positions of the doublet levels.

The parameters derived from the spectra are given in Table 15. Spin—orbit coupling, although important for Co^{2+}, has not been included in any of the calculations for CoF_2. This can lead to an overestimate of Dq, since the spin—orbit components of the ground-state $^4T_{1g}(^4F)$ are spread [79] over about 1000 cm^{-1}, and at cryogenic temperatures transitions will only take place from the lowest populated level, whereas if spin—orbit coupling is neglected the calculated energies correspond to energy differences between the centres of gravity of the spin—orbit components. However the Dq value given by Zimring and Stout [76] is probably reasonably accurate since it was obtained from the energy difference between the first two spin-allowed transitions, which equals 10 Dq, and thus the effect of the spin—orbit splitting of the

TABLE 15

Ligand field parameters for cobalt dihalides (Parentheses indicate source of measurement if different from ref.)

	Ref.	Temp. (K)	Dq (cm^{-1})	B (cm^{-1})	C (cm^{-1})	C/B
CoF_2	75	RT	720	—	—	—
	76	20.4	715	971 [a]	—	—
	77,78	RT	850	—	—	—
	79	2.2	670	—	—	—
$CoCl_2$	75	RT	700	—	—	—
	80	RT	750	766	—	—
	15(81)	20	764	755	—	—
	81 [b]	20	690	780	3432 [c]	4.4 [c]
$CoBr_2$	75	RT	625	—	—	—
	80	RT	697	713	—	—
	15(75)	RT	649	786	—	—
	81 [b]	20	640	760	3344 [c]	4.4 [c]

[a] Free-ion value of B used. [b] Spin—orbit coupling included, ζ = 420 cm^{-1}. [c] C fixed equal to 4.4 B as in free ion.

ground-state is cancelled out. Van der Ziel and Guggenheim [79] obtained their value similarly although the separation between the zero-phonon lines for each transition was fitted rather than the energy difference between the Franck—Condon maxima. It is not clear how Eremenko et al. [77,78] arrived at their value, but it appears to be too high and is probably in error.

Since the energies of the doublet levels have not been calculated, no value of the Racah parameter C is available.

(2) $CoCl_2$ and $CoBr_2$. The room-temperature diffuse reflectance spectra of $CoCl_2$ and $CoBr_2$ have been reported by Ludi and Feitknecht [75] and by Zahner and Drickamer [80] (Table 14). In addition the single-crystal spectra of these two compounds have been recorded at temperatures down to 20 K by Ferguson et al. [81] and the spectra of polycrystalline layers studied down to 77 K by Trutia and Musa [82].

The spin-allowed transition $^4T_{1g}(^4F) \rightarrow {}^4A_{2g}(^4F)$ was not observed in the diffuse reflectance spectrum by Zahner and Drickamer [80] and the single crystal measurements showed that this transition was very weak relative to the spin-allowed transitions to the $^4T_{2g}(^4F)$ and $^4T_{1g}(^4P)$ states. This can be understood qualitatively by considering the strong-field configurations of the states. The configuration of the $^4A_{2g}(^4F)$ level is $t_{2g}{}^3e_g{}^4$ and the ground state is mainly $t_{2g}{}^5e_g{}^2$ and so the transition is effectively a two-electron jump, whereas the configurations of the two other quartet states are $t_{2g}{}^4e_g{}^3$ and thus transitions to these states are one-electron jumps.

Only the highest energy spin-allowed transition to the $^4T_{1g}(^4P)$ state has been observed to show structure, for both $CoCl_2$ and $CoBr_2$, and this has

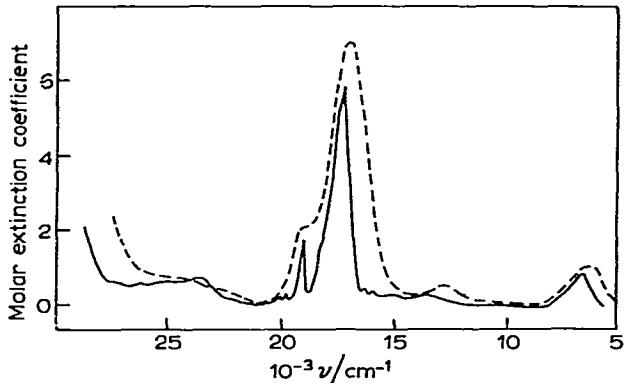

Fig. 7. Absorption spectrum of $CoCl_2$: dashed, room temperature; solid trace, 20 K [81].

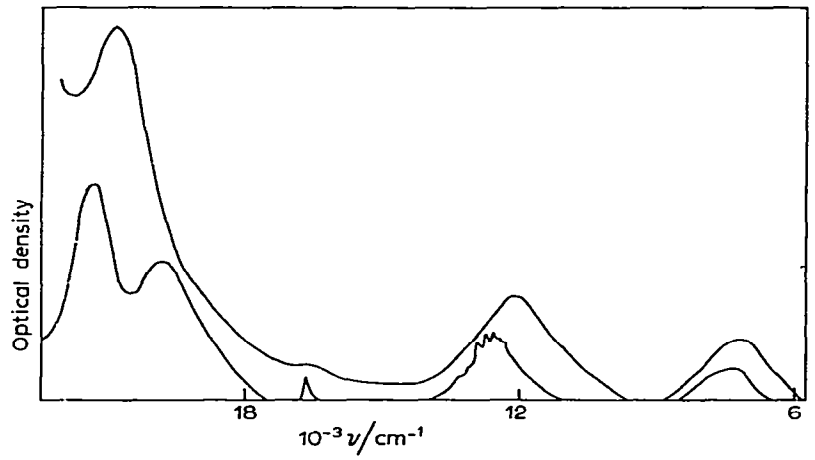

Fig. 8. Absorption spectrum of $NiBr_2$: upper, 300 K; lower, 5 K [91].

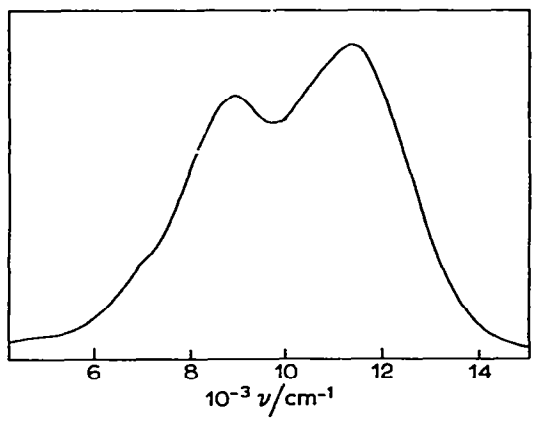

Fig. 9. Reflectance spectrum of CuF_2 at room temperature [102].

been ascribed to spin—orbit splitting [81]. This state has been calculated to have the largest spread of spin—orbit components, $\simeq 500$ cm^{-1} for $CoCl_2$ and $\simeq 425$ cm^{-1} for $CoBr_2$, of all the excited quartet levels [81].

Several spin-forbidden transitions to doublet states were also observed in the crystal spectra and have been assigned by Ferguson et al. [81]. However only the states arising from the ^2H free-ion term were well accounted for by theory for $CoCl_2$, and for $CoBr_2$ agreement between experiment and theory was found to be poor even for these levels. The closeness of the charge-transfer bands in $CoBr_2$ has been suggested as a cause of this poor correspondence and also the fact that the C/B ratio was fixed at the free-ion value, in the theoretical calculations [81]. This assumption of a fixed C/B ratio (contrasting with Ferguson's later approach [12]) is incompatible with the nephelauxetic effect [20]. In addition it must be remembered that the doublet states ^2F, ^2P and ^2D have not been observed in the free ion. It is therefore not known whether they are fitted by the theoretical Slater—Condon—Shortley equations, and hence whether the ligand—field states derived from these terms are expected to be well fitted by theory.

Spin—orbit coupling has only been included in the derivation of parameters from the spectra of $CoCl_2$ and $CoBr_2$ (Table 15) by Ferguson et al. [81] who fitted the 20 K spectra. Thus, in the light of the discussion of the effect of spin—orbit coupling for CoF_2 these are probably the most reliable values for these compounds, but no great reliance should be placed on the Racah parameter C since it was obtained from the free-ion ratio C/B.

(vii) d^8 Nickel dihalides

(1) NiF_2. Nickel difluoride has the tetragonal rutile structure in which each Ni^{2+} ion is surrounded by a distorted octahedron of F^- ions [68]. The octahedron is angularly distorted and elongated such that four Ni—F distances are 2.01 Å and the other two 2.00 Å. Again this distortion is relatively small and the electronic spectrum of NiF_2 can be analysed on the basis of an octahedral ligand field.

The room-temperature diffuse reflectance spectrum of NiF_2 has been recorded by Rüdorff et al. [83] and by Ludi and Feitknecht [75]. The single-crystal spectrum at 300 K has been measured by Balkanski et al. [84] and these authors also recorded selected regions at 85 K. Ferguson et al. [85a] also recorded the single-crystal room-temperature spectrum but, owing to a sample mix-up [85b], the crystal was mistakenly identified as CrF_3 and thus assignments were made on the basis of a d^3 ion in an octahedral field. (Detailed studies have been made of the spin-forbidden $^3A_{2g}(^3F) \rightarrow {}^1T_{2g}(^1D)$ transition in the single-crystal spectrum at temperatures down to 4.2 K, by Belyaeva et al. [86] primarily in connexion with the magnon sidebands).

All the observed spectra are in reasonable agreement, as shown in Table 16, but for some bands there are differing assignments. Ludi and Feitknecht [75] observed a broad band at 12 800 cm^{-1} with a low energy shoulder at

TABLE 16

Observed energy levels (cm^{-1}) relative to $^3A_{2g}(^3F)$ ground state for nickel difluoride

	DR [75] RT	DR [83] RT	SC [84] [c] 300 K	SC [85] [g] RT
$^3T_{2g}(^3F)$	75 000	—	7450 [d,e]	7500
$^3T_{1g}(^3F)$	12 000	12 900	12 270 [d]	13 000
			13 020 [e]	
$^1E_g(^1D)$	12 800 [a]	15 050	15 075 [d]	15 000
			15 220 [e]	
$^1T_{2g}(^1D)$	21 000	21 000	21 300 [d]	21 000
			20 800 [e]	
$^1A_{1g}(^1G)$	23 200 [b]	—	—	22 500 [b]
$^3T_{1g}(^3P)$	24 000	24 100	24 450 [d]	24 000
			24 150 [e]	
$^1T_{1g}(^1G)$	—	28 000	28 200	—
$^1E_g, ^1T_{2g}(^1G)$	—	—	32 000 [f]	—

[a] The assignment of this band is incorrect. It probably arises from transitions to spin—orbit components of the $^3T_{1g}(^3F)$ level. [b] The assignment of the transition to the $^1A_{1g}(^1G)$ must be considered tentative. [c] Bands also observed at 30 150, 36 000, 38 200 cm^{-1}. See text and Table 17 for assignment. [d] Electric vector of polarized light parallel to c axis. [e] Electric vector of polarized light perpendicular to c axis. [f] This assignment from this work. [g] These authors do not give the observed maxima but they are tabulated in ref. 88. The assignments are from this work.

12 000 cm^{-1}. These absorptions were assigned to transitions to the $^1E_g(^1D)$ and $^3T_{1g}(^3F)$ levels respectively, but they most probably arise from transitions to the spin—orbit components of the $^3T_{1g}(^3F)$ level which is split by spin—orbit coupling. The $^3A_{2g}(^3F) \rightarrow {}^1E_g(^1D)$ transition has been calculated [84] to occur at 15 150 cm^{-1} and the absorption observed at $\simeq$15 150 cm^{-1} by Rüdorff et al. [83] and by Balkanski et al. [84] has thus been assigned accordingly.

Ludi and Feitknecht [75] observed a shoulder on the low-energy side of the $^3A_{2g}(^3F) \rightarrow {}^3T_{1g}(^3P)$ transition and assigned it to the $^3A_{2g}(^3F) \rightarrow {}^1A_{1g}(^1G)$ transition. Ferguson et al. [85,87] also observed a weak band at 22 500 cm^{-1} but the other spectra revealed no absorption in this region and so the transition to the $^1A_{1g}(^1G)$ level was not assigned in these cases. This shoulder may arise from the spin—orbit splitting of the $^3T_{1g}(^3P)$ state and thus Ludi and Feitknecht's assignment must be considered tentative.

In the single-crystal spectrum, four bands at 30 150, 32 000, 36 000 and 38 200 cm^{-1}, whose intensity appeared to increase as the temperature was lowered, were observed in the UV region [84]. Only two transitions, to the $^1E_g(G)$ and $^1T_{2g}(G)$ levels, are predicted in this region, and their energies are calculated [84] to be very similar, and so only one observable band might be expected. Thus Balkanski et al. [84] were unable to assign all these absorptions to simple ligand—field transitions.

TABLE 17

Observed and calculated energies of double-exciton transitions in NiF_2 at 300 K

Observed energy (cm^{-1})	Assignment	Calculated energy (cm^{-1})
30 150	$^3A_{2g}(^3F) \rightarrow {}^1E_g(^1D) + {}^1E_g(^1D)$	30 300
36 000	$^3A_{2g}(^3F) \rightarrow {}^1E_g(^1D) + {}^1T_{2g}(^1D)$	36 150
38 200	$^3A_{2g}(^3F) \rightarrow {}^1E_g(^1D) + {}^1A_{1g}(^1G)$	37 650

However, since then Ferguson [87] has studied the UV spectrum of $KNiF_3$ and has observed similar bands which he assigned to double-exciton transitions. These transitions arise from the simultaneous electronic excitation of two Ni^{2+} ions, coupled by exchange interactions, to singlet levels. This process can cause the breakdown of the spin-selection rule and give rise to anomalously intense bands. Thus the absorptions in NiF_2 can a fortiori be described similarly and while the band at 32 000 cm^{-1} should be assigned to the spin-forbidden transition $^3A_{2g}(^3F) \rightarrow {}^1E_g, {}^1T_{2g}(^1G)$ which Balkanski et al. calculated [84] to occur at approximately 32 600 cm^{-1}, the remaining absorptions are then to be assigned to double-exciton transitions as shown in Table 17. Taking the energies of the $^1E_g(^1D)$, $^1T_{2g}(^1D)$ and $^1A_{1g}(^1G)$ levels as 15 150, 21 000 and 22 500 cm^{-1} respectively, the energies of these transitions can be calculated. These calculated positions are shown in Table 17 and are in good agreement with the observed energies.

Ligand field parameters have been derived from the observed spectra by Balkanski et al. [84] and by Ludi and Feitknecht [75], and both sets are in good agreement as shown in Table 20. The reservation should be entered however that the spectra are for ~300 K and not ~0 K.

(2) $NiCl_2$ and $NiBr_2$. The room temperature diffuse reflectance spectra of $NiCl_2$ and $NiBr_2$ have been reported by Bostrop et al. [89,90], Ludi and Feitknecht [75] and by Zahner and Drickamer [80]. Single-crystal spectra at temperatures down to 5 K have been recorded by Ackerman et al. [91] and by Kozielski et al. [92,93]. Their respective assignments are shown in Tables 18 and 19 and these reveal several disagreements. In addition some differences in the spectra are also observed and these will be discussed below for each compound.

(a) $NiCl_2$. The assignment of the lowest energy spin-allowed transition to the $^3T_{2g}(^3F)$ level in $NiCl_2$ is not in dispute. However the 5 K single-crystal spectrum obtained by Kozielski et al. [93] showed four sharp peaks with associated sideband structure in the absorption corresponding to this transition, whereas Ackerman et al. [91] observed no structure in this absorption in their single-crystal spectrum at 5 K. These four peaks have been assigned to transitions to the pure electronic spin—orbit components $^3\Gamma_3$, $^3\Gamma_4$, $^3\Gamma_5$ and $^3\Gamma_2$ of

TABLE 18

Observed energy levels (cm^{-1}) relative to $^3A_{2g}(^3F)$ ground state for nickel dichloride

	DR [89,90] [a] RT	DR [75] [a] RT	DR [80] RT	SC [91] [b] 5 K	SC [92,93] [c] 5 K
$^3T_{2g}(^3F)$	—	7200	7550	7697	≃7600 [d]
$^3T_{1g}(^3F)$	12 900	11 500	12 560	{11 850 12 700	{≃11 800— ≃16 000
$^1E_g(^1D)$	11 600	12 400	—	≃13 850	—
$^1T_{2g}(^1D)$	19 400	19 200	—	—	≃20 000
$^1A_{1g}(^1G)$	—	—	—	20 200	—
$^3T_{1g}(^3P)$	22 100	21 900	—	22 600	≃22 600
$^1T_{1g}(^1G)$	—	—	—	—	≃27 000
^1E_g, $^1T_{2g}(^1G)$	—	—	—	27 200	≃30 000

[a] Some mistranscription appears to have crept into the quotation of the data of refs. 89, 90 in ref. 75. [b] Absorption also observed at 30 200 cm^{-1} but was not assigned. [c] These authors have not tabulated the maxima of all the observed absorptions, and so most of the energies given here have been estimated from the diagrams of the spectra. [d] Sharp lines corresponding to transitions to the pure electronic spin—orbit components $^3\Gamma_3$, $^3\Gamma_4$, $^3\Gamma_5$ and $^3\Gamma_2$ of the $^3T_{2g}(^3F)$ state observed at 6519, 6779, 7407 and 7663 cm^{-1} respectively.

the $^3T_{2g}(^3F)$ level [93]. However the separation of the $^3\Gamma_3$ and $^3\Gamma_2$ components is 1150 cm^{-1} which is much larger than the separation observed in the analogous cases of $KNiF_3$, $KZn(Ni)F_3$ and $KMg(Ni)F_3$, where [94,95] it is ≃700 cm^{-1}. In order to reproduce the observed positions of the four components, a large value of the spin—orbit coupling constant ζ is required in the

TABLE 19

Observed energy levels (cm^{-1}) relative to $^3A_{2g}(^3F)$ ground state for nickel dibromide

	DR [89,90] RT	DR [75] RT	DR [80] RT	SC [91] 5 K	SC [92,93] [a] 5 K
$^3T_{2g}(^3F)$	—	6800	7280	7540	≃7400 [b]
$^3T_{1g}(^3F)$	12 100	11 800	12 000	{≃12 300—	{≃10 500— ≃13 500
$^1E_g(^1D)$	10 300	10 200	—	≃13 300	≃16 600
$^1T_{2g}(^1D)$	16 800	17 500	—	≃16 650	≃20 000
$^1A_{1g}(^1G)$	—	20 000	—	≃20 000	—
$^3T_{1g}(^3P)$	20 700	20 600	—	≃21 000	≃21 400

[a] These authors have not tabulated the maxima of all the observed absorptions and so most of the energies given here have been estimated from the diagrams of the spectra. [b] A sharp line observed at 6390 cm^{-1} was assigned to the transition to the pure electronic spin—orbit component $^3\Gamma_3$ of the $^3T_{2g}(^3F)$ state.

theoretical calculations. The value used to give the best fit was [93] $\zeta = 820$ cm^{-1}, unusually larger than the free-ion value [94] of $\zeta = 668$ cm^{-1}, a reduction of the spin—orbit coupling constant being normally expected.

Both the 5 K single-crystal spectra show a broad absorption at 11 000—15 000 cm^{-1}. Two broad humps were observed at $\simeq$11 800 cm^{-1} and 12 700 cm^{-1}, and a highly structured repetitive pattern was found on the high-energy side of the absorption from $\simeq$13 000—14 500 cm^{-1}. Kozielski et al. [93] assigned the two low-energy humps to transitions to the $^3\Gamma_1$ and $^3\Gamma_4$ spin—orbit components of the $^3T_{1g}(^3F)$ state. The structured system was considered to arise from various phonon and magnon modes based on the transition to the $^3\Gamma_5$ component. In addition a broad low intensity band was observed at $\simeq$16 000 cm^{-1} and was assigned to the transition to the $^3\Gamma_3$ component, but this absorption was not observed by Ackerman et al. [91]. However, these assignments are almost certainly incorrect since the spin—orbit splitting of the $^3T_{1g}(^3F)$ state is not expected to be so large. Those given by Ackerman et al. [91] appear to be more appropriate and in accordance with theoretical calculations and with assignments made for related Ni^{2+} compounds such as $CsNiCl_3$, which has a qualitatively very similar spectrum [96]. They [91] assigned the two low energy humps to the transition to the $^3T_{1g}(^3F)$ state, which is split by the spin—orbit coupling. The system of sharp bands was assigned to the spin-forbidden transition $^3A_{2g}(^3F) \rightarrow {}^1E_g(^1D)$ which was calculated by them to occur at $\simeq$13 600 cm^{-1}.

There is also disagreement about the assignment of the spin-forbidden transitions to the $^1T_{2g}(^1D)$, $^1A_{1g}(^1G)$, $^1T_{1g}(^1G)$ and ^1E_g, $^1T_{2g}(^1G)$ levels. A weak structureless band at $\simeq$19 000 cm^{-1} which shifts to $\simeq$20 000 cm^{-1} at 5 K has been assigned to the $^3A_g(^3F) \rightarrow {}^1T_{2g}(^1D)$ transition [75,89,90,92,93]. However, Ackerman et al. [91] assigned this band to the $^3A_{2g}(^3F) \rightarrow {}^1A_{1g}(^1G)$ transition. The former assignment is probably correct since the transition to the $^1T_{2g}(^1D)$ state is calculated to occur in this region and the absorption is generally similar to that observed for this transition in NiF_2. The transition has been observed to show an appreciable increase in intensity as the temperature is lowered. This phenomenon has been explained by Kozielski et al. [92] who proposed a cooperative intensity mechanism which can relax the spin-selection rules, and attributed the broadness of the absorptions to a strong electron—magnon interaction.

Absorptions at $\simeq$27 000 cm^{-1} and $\simeq$30 000 cm^{-1} were observed in the 5 K single-crystal spectra. The higher energy band is remarkably intense for a spin-forbidden transition and at 5 K is the strongest in the ligand—field spectrum. This anomalous intensity has been explained [92] as for the $^3A_{2g}(^3F) \rightarrow {}^1T_{2g}(^1D)$ transition (but Ackerman et al. [91] concluded that a different mechanism is responsible). This higher-energy band has been assigned to the transition to the ^1E_g, $^1T_{2g}(^1G)$ levels and the band at $\simeq$27 000 cm^{-1} to the $^3A_{2g}(^3F) \rightarrow {}^1T_{1g}(^1G)$ transition [92,93]. These assignments appear to be correct, although Ackerman et al. [91] assigned the lower energy band to the $^3A_{2g}(^3F) \rightarrow {}^1E_g$, $^1T_{2g}(^1G)$ transition, and considered that the 30 200 cm^{-1} ab-

sorption is not a single ligand–field transition which omits consideration of any transition to the $^1T_{1g}(^1G)$ level.

(b) $NiBr_2$. The situation regarding the assignment of the electronic spectrum of $NiBr_2$ is just as confused as for $NiCl_2$, though the onset of charge transfer absorption at $\simeq$23 000 cm^{-1} reduces the number of observable bands to discuss.

The lowest-energy band whose Franck–Condon maximum occurs at $\simeq$7300 cm^{-1} at 5 K, has been assigned to the spin-allowed $^3A_{2g}(^3F) \rightarrow {}^3T_{2g}(^3F)$ transition in every case. A sharp line at 6390 cm^{-1} was observed in this absorption at 5 K by Kozielski et al. [93] and was assigned to the transition to the pure electronic spin–orbit component $^3\Gamma_3$ of the $^3T_{2g}(^3F)$ state.

A broad absorption which is highly structured on the high-energy side, was observed in the 11 500–13 500 cm^{-1} region in the 5 K single crystal spectra. In addition one of the crystal spectra [93] showed a weak hump at $\simeq$10 300 cm^{-1} but this was not present in the spectrum obtained by Ackerman et al. [91]. The room temperature diffuse reflectance spectra show a broad band maximum $\simeq$12 000 cm^{-1}, with a shoulder at $\simeq$10 300 cm^{-1}. Transitions to the $^3T_{1g}(^3F)$ and $^1E_g(^1D)$ states are expected to occur in this region and these are generally considered responsible for these absorptions. However there is disagreement as to which level lies highest but it would appear most likely that the assignments given by Ackerman et al. [91] are correct. They have assigned the sharp lines to the transition to the $^1E_g(^1D)$ state, which is coupled to various phonon modes, and consider the $^3A_{2g}(^3F) \rightarrow {}^3T_{1g}(^3F)$ transition to be responsible for the lower energy absorption.

Kozielski et al. [93] assigned all the absorption in this region to the $^3A_{2g}(^3F) \rightarrow {}^3T_{1g}(^3F)$ transition and tentatively assigned the $^3A_{2g}(^3F) \rightarrow {}^1E_g(^1D)$ transition to the series of sharp lines observed at $\simeq$16 600 cm^{-1}. This latter assignment must be extremely doubtful since the $^1E_g(^1D)$ state in $NiBr_2$ is not expected to occur at a higher energy than the corresponding state in NiF_2. This absorption has been assigned to the transition to the $^1T_{2g}(^1D)$ state by the other authors [75,89–91] but is probably best assigned to the $^3T_{2g}(^3F) \rightarrow {}^1A_{1g}(^1G)$ transition.

The other band whose assignment is in dispute occurs at $\simeq$20 000 cm^{-1}. The intensity of this absorption increases markedly as the temperature is decreased and this behaviour has been explained by Kozielski et al. [92] as for the transitions to $^1T_{2g}(^1D)$ and $^1T_{2g}$, $^1E_g(^1G)$ states in $NiCl_2$. By comparison with the similar absorptions observed in NiF_2 and $NiCl_2$, this band seems best assigned to the $^3A_{2g}(^3F) \rightarrow {}^1T_{2g}(^1D)$ transition, but it has also been assigned to the $^3A_{2g}(^3F) \rightarrow {}^1A_{1g}(^1G)$ transition [75,91].

(c) Parameters. The parameters derived from the spectra of $NiCl_2$ and $NiBr_2$ are shown in Table 20. Those derived from the room temperature spectra are in reasonable agreement, and the variation can be ascribed to the usual differences in observed DR band positions. However, the parameter values, obtained by fitting the 5 K spectra, as given by Kozielski et al. [93] and by Ackerman et al. [91], differ considerably. The reason for this discrepancy can be

TABLE 20

Ligand field parameters for nickel dihalides

	Ref.	Temp. (K)	Dq (cm^{-1})	B (cm^{-1})	C (cm^{-1})	C/B
NiF_2	75	RT	750	960	—	—
	84	300	745	965	4053	4.2
$NiCl_2$	75	RT	720	760	—	—
	89, 90	RT	760	750	—	—
	80	RT	755	823	—	—
	91 [a]	5	770	750	3150	4.2
	93 [b]	4.2	692	819	3185 [c]	3.9 [c]
$NiBr_2$	75	RT	680	740	—	—
	89, 90	RT	730	730	—	—
	80	RT	728	730	—	—
	91 [a]	5	740	650	3150	4.85
	93 [b]	4.2	680	765	2975 [c]	3.9 [c]

[a] Spin—orbit coupling included $\zeta = 250\ cm^{-1}$. [b] Spin—orbit coupling included $\zeta = 820\ cm^{-1}$ for $NiCl_2$, $\zeta = 780\ cm^{-1}$ for $NiBr_2$. [c] C/B ratio fixed at 3.9.

traced to the different methods of analysis which were used. Thus, Ackerman et al. [91] fixed the values of Dq and B by fitting to the Franck—Condon maxima of the observed spin-allowed transitions, whereas Kozielski et al. [93] calculated their values by fitting to the observed or estimated positions of the zero-phonon lines of the spin-allowed transitions. Since ligand field theory is best applied to the energies of "vertical" transitions the parameters given by Ackerman et al. [91] are probably preferable.

The values of the Racah parameter C, given by both sets of workers, are not very reliable, due to the uncertainty in the assignment of the spin-forbidden transitions, and also because in one case [93] the value of C was fixed from the free-ion C/B ratio.

(viii) d^9 Copper dihalides (CuF_2, $CuCl_2$ and $CuBr_2$)

The d^9 configuration gives rise to only one free-ion term ^2D, and this is split in an octahedral field into the levels ^2E_g and $^2T_{2g}$ in order of increasing energy. However since the octahedral ground state is ^2E_g it is subject to considerable Jahn—Teller distortion in order to remove the degeneracy of this term. Consequently CuF_2, $CuCl_2$ and $CuBr_2$ have appreciably tetragonally distorted structures.

CuF_2 has a distorted rutile-type structure [97] and $CuCl_2$ [98] and $CuBr_2$ [99] have structures in which infinite chains of planar CuX_4 groups are arranged such that each copper atom has a grossly distorted octahedron of halide ions. In all these compounds the distortion takes the form of an elongation of the CuX_6 octahedra such that the two axial Cu—X bonds are consider-

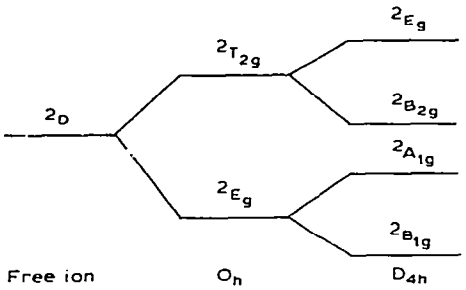

Fig. 3. Splitting of d^9 ^2D term in O_h and D_{4h} (elongated along z axis) ligand fields. (Not to scale). The $^2A_{1g}$ state may lie above the $^2B_{2g}$ or ^2E_g states depending on the degree of distortion.

ably longer than the four equatorial bonds. The degree of distortion is about the same for $CuCl_2$ and $CuBr_2$, and is greater for both these compounds than for CuF_2. For the purposes of the assignment of their electronic spectra the symmetry of these halides may be considered to be D_{4h}.

The octahedral terms ^2E_g and $^2T_{2g}$ are split in a D_{4h} ligand field, as shown in Fig. 3. Since the tetragonal distortion in the copper dihalides takes the form of an elongation of the octahedron, the $^2B_{1g}$ term is considered [39] to be the ground state. Thus three-spin allowed transitions from the $^2B_{1g}$ state to the other doublet states are to be expected and their energies in terms of Dq, Ds and Dt are given by the expressions tabulated for CrF_2 in Table 4, if the multiplicities of the states are ignored. These are the only ligand field transitions, the only free ion state being ^2D.

Only room-temperature diffuse reflectance spectra have been reported for the copper dihalides. Ludi and Feitknecht [100] and also Schmitz-Du Mont and Grimm [101] observed a broad band with two maxima in the near-IR spec-

TABLE 21

Observed maxima (cm^{-1}) and assignments for room-temperature spectra of copper dihalides

Compound	$^2B_{1g} \rightarrow {}^2A_{1g}$	$^2B_{1g} \rightarrow {}^2B_{2g}$	$^2B_{1g} \rightarrow {}^2E_g$	Unassigned bands	Ref.
CuF_2 [a]	7500	8800	11 350	—	39, 102 [b]
	—	8850	11 400	—	101
	- -	8800	11 400	—	100
$CuCl_2$	—	12 200		—	103
	—	—	—	8500, 11 800	100
$CuBr_2$	—	—	—	8000, 9300	100

[a] Assignments for CuF_2 due to Oelkrug [39,102]. [b] Derived values of splitting-parameters; Dq = 88[illegible] cm^{-1}, Ds = 1435 cm^{-1}, Dt = 350 cm^{-1}.

trum of CuF_2. However Oelkrug [39,102] resolved a further band on the low energy side of the two maxima by decomposing the broad absorption into Gaussian components and was thus able to assign all three spin-allowed transitions and hence derive the values of the splitting parameters. The observed maxima and assignments are shown in Table 21.

The diffuse reflectance spectrum of $CuCl_2$ has been recorded by Hatfield and Piper [103] and Ludi and Feitknecht [100] who also recorded the spectrum of $CuBr_2$. A broad band was observed for both compounds and Ludi and Feitknecht were able to resolve it into two components for $CuCl_2$ and $CuBr_2$, but Hatfield and Piper [103] only found one for $CuCl_2$. The observed maxima are shown in Table 21, but they are not considered to be very reliable, particularly for the dibromide, due to the close proximity of charge transfer bands [100].

REFERENCES

1 C.K. Jørgensen, Absorption Spectra and Chemical Bonding in Complexes, Pergamon Press, Oxford, 1962.
2 C.K. Jørgensen, Progr. Inorg. Chem., 4 (1962) 73
3 C.K. Jørgensen, Struct. Bonding, 1 (1966) 3.
4 M. Gerloch and R.C. Slade, Ligand—Field Parameters, University Press, Cambridge, 1973.
5 N.S. Hush and M.H.L. Pryce, J. Chem. Phys., 28 (1958) 244.
6 N.S. Hush, Discuss. Faraday Soc., 26 (1958) 145.
7 W.G. Penney, Trans. Faraday Soc., 35 (1940) 627.
8 L.E. Orgel, J. Chem. Soc., (1952) 4756.
9 P. George and D.S. McClure, Progr. Inorg. Chem., 1 (1959) 381.
10 D.S. McClure, Solid State Phys., 9 (1959) 399.
11 N.S. Hush and R.J. Hobbs, Progr. Inorg. Chem., 10 (1968) 259.
12 J. Ferguson, Progr. Inorg. Chem., 12, (1970) 159.
13 J.S. Griffith, The Theory of Transition-Metal Ions, University Press, Cambridge, 1961.
14 C.J. Ballhausen, Introduction to Ligand Field Theory, McGraw-Hill, New York, 1962.
15 A.B.P. Lever, Inorganic Electronic Spectroscopy, Elsevier, Amsterdam, 1968; J. Chem. Educ., 45 (1968) 711.
16 R. Colton and J.H. Canterford, Halides of the First Row Transition Metals, Wiley-Interscience, London, 1969.
17 B.N. Figgis, Introduction to Ligand Fields, Wiley-Interscience, London, 1967.
18 E. König, Struct. Bonding, 9 (1971) 175.
19 E. König, Z. Naturforsch. B, 27 (1972) 1.
20 H. Witze, Theor. Chim. Acta, 20 (1971) 171.
21 J. Ferguson, H.J. Guggenheim and E.R. Krausz, Aust. J. Chem., 22 (1969) 1809.
22 J. Ferguson, Aust. J. Chem., 21 (1968) 307.
23 J. Ferguson and D.L. Wood, Aust. J. Chem., 23 (1970) 861.
24 J. Ferguson, Aust. J. Chem., 23 (1970) 635.
25 V.V. Eremenko and A.I. Belyaeva, Sov. Phys.-Uspekhi, 12 (1969) 320.
26 D.D. Sell, R.L. Greene and R.M. White, Phys. Rev., 158 (1967) 489.
27 D.D. Sell, J. Appl. Phys., 39 (1968) 1030.
28 H.M. Crosswhite and H.W. Moos (Eds.), Optical Properties of Ions in Crystals, Interscience, New York, 1967.

29 B. DiBartolo (Ed.), Optical Properties of Ions in Solids, Plenum Press, New York, 1975.
30 R.J.H. Clark, J. Chem. Soc., (1964) 417.
31 G.W.A. Fowles, T.E. Lester and R.A. Walton, J. Chem. Soc. (A), (1968) 1081.
32 W.E. Smith, J. Chem. Soc. (A), (1969) 2677.
33 W.E. Smith, J. Chem. Soc. Dalton, (1972) 1634.
34 S.S. Kim, S.A. Reed and J.W. Stout, Inorg. Chem., 9 (1970) 1584.
35 W. van Erk and C. Haas, Phys. Status Solidi B, 71 (1975) 537.
36 L.L. Lohr and D.S. McClure, J. Chem. Phys., 49 (1968) 3516.
37 J.P. Fackler and D.G. Holah, Inorg. Chem., 4 (1965) 954.
38 D. Oelkrug, Ber. Bunsenges. Phys. Chem., 70 (1966) 736.
39 D. Oelkrug, Struct. Bonding, 9 (1971) 1.
40 P.E. Lim and J.W. Stout, J. Chem. Phys., 63 (1975) 4886.
41 W.W. Holloway and M. Kestigan, Spectrochim. Acta, 22 (1966) 1381.
42 K.H. Jack and R. Maitland, Proc. Chem. Soc., (1957) 232.
43 A.D. Liehr and C.J. Ballhausen, Ann. Phys. (N.Y.), 3 (1958) 304.
44 J.W. Cable, M.K. Wilkinson and E.O. Wollan, Phys. Rev., 118 (1960) 950.
45 J.W. Tracey, N.W. Gregory, E.C. Lingafelter, J.D. Dunitz, H.C. Mez, R.E. Scheringer, H.Y. Yakel and M.K. Wilkinson, Acta Crystallogr., 14 (1961) 927.
46 H.R. Oswalt, Helv. Chim. Acta, 44 (1961) 1049.
47 J.W. Stout, J. Chem. Phys., 31 (1959) 709.
48 J.W. Stout, J. Chem. Phys., 33 (1960) 303.
49 R. Pappalardo, J. Chem. Phys., 31 (1959) 1050.
50 R. Pappalardo, J. Chem. Phys., 33 (1960) 613.
51 H.J. Hrostowski and R.H. Kaiser, Bull. Am. Phys. Soc., 4 (1959) 167.
52 D.M. Finlayson, I.S. Robertson, T. Smith and R.W.H. Stephenson, Proc. Phys. Soc., 76 (1960) 355.
53 R. Stevenson, Can. J. Phys., 43 (1965) 1732.
54 J.J. Foster and N.S. Gill, J. Chem. Soc. (A), (1968) 269.
55 A. Mehra, J. Chem. Phys., 48 (1968) 1871.
56 W. van Erk and C. Haas, Phys. Status Solidi B, 70 (1975) 517.
57 M. Régis and Y. Farge, J. Phys. (Paris), 37 (1976) 627.
58 Y. Farge, M. Régis and B.S.H. Royce, J. Phys. (Paris), 37 (1976) 637.
59 T. Fujiwara, W. Gebhardt, K. Petanides and Y. Tanabe, J. Phys. Soc. Jap., 33 (1972) 39.
60 W. Low and G. Rosengarten, J. Mol. Spectrosc., 12 (1964) 319.
61 Y. Tanabe and S. Sugano, J. Phys. Soc. Jap., 9 (1954) 753.
62 D. Curie, C. Barthou and B. Canny, J. Chem. Phys., 61 (1974) 3048.
63 B.R. Russell and R.M. Hedges, Theor. Chim. Acta, 19 (1970) 335.
64 J. Tylicki and W.M. Yen, Phys. Rev., 166 (1968) 488.
65 G.D. Jones, Phys. Rev., 155 (1967) 259.
66 H. Brokopf, D. Reinen and O. Schmitz-Du Mont, Z. Phys. Chem. N.F., 68 (1969) 228.
67 W.E. Hatfield and T.S. Piper, Inorg. Chem., 3 (1964) 1295.
68 W.H. Baur, Acta Crystallogr., 11 (1958) 488.
69 G. Winter, Aust. J. Chem., 21 (1968) 2859.
70 S.E. Schnatterly and M. Fontana, J. Phys. (Paris), 33 (1972) 691.
71 T.E. Freeman and G.D. Jones, Phys. Rev., 182 (1969) 411.
72 D.J. Robbins and P. Day, Chem. Phys. Lett., 19 (1973) 529.
73 J.A. Griffin, S.E. Schnatterly, Y. Farge, M. Régis and M.P. Fontana. Phys. Rev. B, 10 (1974) 1960.
74 D.J. Robbins and P. Day, J. Phys. C, Sol. Stat. Phys., 9 (1976) 867.
75 A. Ludi and W. Feitknecht, Helv. Chim. Acta, 46 (1963) 2226.
76 L.J. Zimring and J.W. Stout, J. Chem. Phys., 51 (1969) 4197.

77 V.V. Eremenko and A.I. Zvyagin, Sov. Phys., Solid State, 6 (1964) 782.
78 V.V. Eremenko and A.I. Belyaeva, Sov. Phys., Solid State, 6 (1965) 2918.
79 J.P. van der Ziel and H.J. Guggenheim, Phys. Rev., 166 (1968) 479.
80 J.C. Zahner and H.G. Drickamer, J. Chem. Phys., 35 (1961) 1484.
81 J. Ferguson, K. Knox and D. Wood, J. Chem. Phys., 39 (1963) 881.
82 A. Trutia and M. Musa, Phys. Status Solidi, 8 (1965) 663.
83 W. Rüdorff, J. Kändler and D. Babel, Z. Anorg. Allgem. Chem., 317 (1962) 261.
84 M. Balkanski, P. Moch and R.G. Shulman, J. Chem. Phys., 40 (1964) 1897.
85 J. Ferguson, K. Knox and D.L. Wood, J. Chem. Phys., (a) 35 (1961) 2236; (b) Erratum, 37 (1962) 193.
86 A.I. Belyaeva, V.V. Eremenko, N.N. Mikhailov, V.N. Pavlov and S.V. Petrov, Sov. Phys., JETP., 23 (1966) 979.
87 J. Ferguson, Aust. J. Chem., 21 (1968) 323.
88 A.D. Liehr, J. Phys. Chem., 67 (1963) 314.
89 R.W. Asmussen and O. Bostrop, Acta Chem. Scand., 11 (1957) 745.
90 O. Bostrop and C.J. Jorgensen, Acta Chem. Scand., 11 (1957) 1223.
91 J. Ackerman, C. Fouassier, E.M. Holt and S.L. Holt, Inorg. Chem., 11 (1972) 3118.
92 M. Kozielski, I. Pollini and G. Spinolo, Phys. Rev. Lett., 27 (1971) 1223.
93 M. Kozielski, I. Pollini and G. Spinolo, J. Phys. C, Sol. Stat. Phys., 5 (1972) 1253.
94 J. Ferguson, H.J. Guggenheim and D.L. Wood, J. Chem. Phys., 40 (1964) 822.
95 J. Ferguson and H.J. Guggenheim, J. Chem. Phys., 44 (1966) 1095.
96 G.L. McPherson and G.D. Stucky, J. Chem. Phys., 57 (1972) 3780.
97 C. Billy and H.M. Haendler, J. Am. Chem. Soc., 79 (1957) 1049.
98 A.F. Wells, J. Chem. Soc., (1947) 1670.
99 L. Helmholtz, J. Am. Chem. Soc., 69 (1947) 886.
100 A. Ludi and W. Feitknecht, Helv. Chim. Acta, 46 (1963) 2238.
101 O. Schmitz-Du Mont and D. Grimm, Z. Anorg. Allgem. Chem., 355 (1967) 280.
102 D. Oelkrug, Z. Phys. Chem. N.F., 56 (1967) 325.
103 W. Hatfield and T. Piper, Inorg. Chem., 3 (1964) 841.
104 J.C. Slater, Quantum Theory and Atomic Structure, Vols. I and II, McGraw-Hill, New York, 1960.
105 W. Klemm and L. Grimm, Z. Anorg. Allgem. Chem., 249 (1941) 209.
106 P.G. Russell, D.S. McClure and J.W. Stout, Phys. Rev. Lett., 16 (1966) 176.
107 G. Racah, Phys. Rev., 85 (1952) 381.
108 S. Koide and M.H.L. Pryce, Phil. Mag., 3 (1958) 607.
109 J. Lee and A.B.P. Lever, J. Mol. Spectrosc., 26 (1968) 189.